https://ntrs.nasa.gov/search.jsp?R=19930082177 2020-06-17T20:55:54+00:00Z

Y 3.N21/5:6/1310

GOVT. DOC.

NATIONAL ADVISORY COMMITTEE FOR AERONAUTICS

TECHNICAL NOTE

No. 1310

CHARTS FOR STRESS ANALYSIS OF REINFORCED CIRCULAR CYLINDERS UNDER LATERAL LOADS

By Joseph Kempner and John E. Duberg

Langley Memorial Aeronautical Laboratory
Langley Field, Va.

Washington

May 1947

BUSINESS, SCIENCE & TECHNOLOGY DEP'T.
JUN 4 1947

629.1309
Un34

ERRATUM

NACA TN 1310

CHARTS FOR STRESS ANALYSIS OF REINFORCED CIRCULAR CYLINDERS UNDER LATERAL LOADS

By Joseph Kempner and John E. Duberg

May 1947

Figure 40: When the curves for C_{st_0} in this figure were faired in between the computed points, the fairings for values of A/B of 30 and 100 were inadvertently reversed in the cross-over region near $\phi = 42^\circ$. These curves should be identical, except for sign, with those for C_{mr_0} in figure 33, for which the fairings are correct. Values of the coefficient C_{st_0} can therefore be obtained from the latter curves with signs reversed.

CONN. STATE LIBRARY
NOV 1 1950

NACA-Langley - 10-26-50 - 775

NATIONAL ADVISORY COMMITTEE FOR AERONAUTICS

TECHNICAL NOTE NO. 1310

CHARTS FOR STRESS ANALYSIS OF REINFORCED CIRCULAR CYLINDERS UNDER LATERAL LOADS

By Joseph Kempner and John E. Duberg

SUMMARY

Charts providing coefficients for the stress analysis of a reinforced circular cylinder are presented. These charts facilitate the rapid determination of the shear flows and direct stresses in the sheet of the cylinder as well as the shear forces, axial forces, and bending moments in the rings. Separate charts are given for each of the three basic ring loadings: a concentrated radial load, a concentrated tangential load, and a concentrated bending moment. These charts apply to a cylinder of uniform construction loaded in the plane of one reinforcing ring and are based upon the solution of the finite-difference equation developed in NACA Technical Note No. 1219, which, in contrast to the elementary engineering analysis, includes the effects of deformations of rings and sheet. To obtain the coefficients the stress analyst need merely compute the values of two simple structural parameters and refer to the curves presented in the charts. The stresses due to loads applied at several rings or at different positions on the same ring can be superimposed to give the stresses caused by these loads acting simultaneously.

INTRODUCTION

In several papers (references 1 to 4) the elementary theory of bending and torsion is shown to be inadequate for the stress analysis of the relatively flexible shell structures used in airframe construction. In reference 1 a recurrence formula suitable for an accurate analysis of the stresses in reinforced circular cylinders was developed. This formula was treated for long cylinders (similar to airplane fuselages) as a fourth-order finite-difference equation and was readily solved for cylinders of uniform construction. The present paper contains charts based on the solution of the finite-difference equation. These charts enable the stress analyst to determine the stresses and loads in the sheet and rings of either a long or a relatively short cylinder in the vicinity of external forces.

SYMBOLS

$A = \frac{R^6 t'}{IL^3}$

$B = \frac{Et'R^2}{GtL^2}$

$\frac{A}{B} = \frac{GtR^4}{EIL}$

C	coefficient of load or stress
E	Young's modulus
G	shear modulus
H_ϕ	axial force in ring at angle ϕ
I	moment of inertia of cross section of ring
L	length of bay
M_O	concentrated bending moment on ring 0 at $\phi = 0^\circ$
M_ϕ	bending moment in ring at angle ϕ
P_O	radial load on ring 0 at $\phi = 0^\circ$
R	radius of cylinder and ring
T_O	tangential load on ring 0 at $\phi = 0^\circ$
V_ϕ	shear force in ring at angle ϕ
q_ϕ	shear flow in skin at angle ϕ
q_R	elementary shear flow in skin at angle ϕ (corresponds to shear flow for $\frac{A}{B} = 0$)
t	thickness of skin
t'	thickness of all material carrying bending stresses in cylinder if uniformly distributed around perimeter (effective skin)

σ_ϕ longitudinal direct stress in effective skin at ring stations and at angle ϕ

ϕ angular coordinate of point on cylinder

Subscripts:

a axial force in ring

m bending moment in or on ring

q shear flow in skin

r radial load on ring

s shear force in ring

t tangential load on ring

σ direct stress in effective skin at ring stations

$\Delta\sigma$ direct correction stress in effective skin at ring stations

-1, 0, 1 designation of ring or bay

When double subscripts appear, first subscript indicates loads or stresses in structural component, and second, applied loading on the cylinder.

BASIS FOR DESIGN CHARTS

The theory upon which the design charts are based is presented in detail in reference 1. Essentially, the analysis consists of the development and solution in closed form of a fourth-order finite-difference equation. The development is based upon the maintenance of continuity of deformations between reinforcing rings and sheet of a circular semimonocoque cylinder. Only external forces acting in the plane of the ring are considered. The coordinate conventions are given in figure 1 and the sign conventions for forces and stresses in figure 2.

Basic assumptions.- In the development of the theory of reference 1 the following basic assumptions were made:

(1) The structure considered is a circular cylinder consisting of bays of identical construction and extending longitudinally to infinity in both directions from a loaded ring. (See fig. 1.)

(2) The reinforcing rings are of constant moment of inertia and are attached continuously to the periphery of the sheet. The radius to the neutral axis of each ring coincides with the radius of the middle surface of the sheet.

(3) The part of the sheet area which is considered to resist bending stresses is added to the stringer area and the combination is uniformly distributed about the periphery of the cylinder. This resulting combination is an effective skin thickness t' which resists direct stresses. The actual sheet area is considered capable of supporting only shear stresses.

(4) Young's modulus E and the shear modulus G are constant throughout the cylinder. Poisson's ratio is zero.

(5) Radial deformation of rings and sheet cause no circumferential extension of these elements.

In accordance with assumption (3), the shear stresses in the skin do not vary longitudinally except at rings.

Applicability of theory to cylinders of finite length.- Although the solution of the finite-difference equation is exact only for infinitely long cylinders, it is shown in reference 1 that the stresses and loads determined from this solution compare favorably with those obtained from experiment and from an exact analysis for cylinders of finite length, provided that the cylinders are loaded at least two bays from external restraints. The good agreement indicated follows from the fact that whereas a concentrated load causes distortions in the region of the load, the part of the cylinder located a few bays from the load can be assumed undisturbed.

APPLICATION OF DESIGN CHARTS

Scope and use of charts.- In reference 1 it is shown that calculations of the stresses and loads in reinforced cylinders consistent with the preceding assumptions are dependent only upon

the loads introduced and the structural parameters $A = \frac{R^6 t'}{IL^3}$ and $\frac{A}{B} = \frac{GtR^4}{EIL}$. Values for the design charts (figs. 3 to 47) were, consequently, computed by use of the formulas of reference 1. Formulas shown in the figures are defined in table 1. For given values of the structural parameters A and A/B, the stress analyst can use the charts to determine the following stresses and loads at any point on the periphery of a cylinder:

(1) The shear flows in the sheet of the bays adjacent to the loaded ring

(2) The direct stresses in the effective skin at the loaded ring and at the two rings adjacent to this ring

(3) The moments, shears, and axial forces in the loaded ring and the two adjacent rings

To apply the charts the stress analyst must compute the values of the structural parameters A and A/B and refer to the curves which most nearly correspond to these two values. (See appendix.) For each of the values of $A = 2 \times 10^2$, 2×10^4, and 2×10^6, curves are presented corresponding to several values of A/B ranging from 0 to ∞. The stresses and loads in the sheet and rings are determined from the formulas and curves given in the charts.

Application to cantilevered cylinders.- Separate charts are presented for each of the three basic ring loadings: a concentrated radial load, a concentrated tangential load, and a concentrated bending moment. These charts apply directly to cantilevered cylinders loaded in the plane of one reinforcing ring. The stresses and loads caused by two or more of the basic ring loadings can be combined to give the stresses and loads resulting from any type of applied concentrated load. The stresses due to loads acting at several rings at various angles ϕ can be superimposed to give the stresses caused by these loads acting simultaneously.

Application to cylinders not cantilevered.- Although the charts are constructed upon the assumption that the cylinders are cantilevered, they nevertheless can be used in the analysis of cylinders not cantilevered. As indicated in reference 1, stresses and loads in the sheet and rings of a cantilevered or noncantilevered cylinder

can be resolved into the following two components: (1) the equilibrium stresses and loads obtained from the elementary theory of bending and torsion (reference 5) and (2) the correction stresses and loads due to the consideration of the distortions of rings and sheet.

In the charts presented the coefficients for the elementary stresses and loads are those of a cantilevered circular cylinder and correspond to the curve for $\frac{A}{B} = 0$ in each chart. For other conditions of support the charts for ring coefficients are valid in their present form, whereas those for sheet coefficients are readily applied if, for each loading condition, coefficients for $\frac{A}{B} = 0$ are subtracted from the coefficients corresponding to the values of A and A/B pertinent to the cylinder being analyzed. The resulting differences represent correction coefficients which can be added to the elementary values consistent with any other type of end restraint. (See appendix for a numerical example.)

ACCURACY OF CHARTS

It was shown in reference 1 that the method of analysis applied in the construction of the design charts can be expected to give stresses and loads which agree satisfactorily with experimental values, provided that the external restraints on the cylinder being analyzed are located two or more bays from the loaded ring. The numerical example given in reference 1, however, utilizes exact values of A and A/B for the cylinder analyzed. Since, in general, these values for a particular cylinder will not correspond exactly to any of the curves presented in figures 3 to 47, a numerical example, in which values of A and A/B from the charts are used, is given in the appendix. The curves in figures 48 and 49 show comparisons among some of the coefficients for a radially loaded cylinder obtained by using chart values, by recurrence-formula solution based on the finite cylinder as in reference 1, by the standard or elementary solution, and by experiment (cylinder 2, reference 4). Although the cylinder analyzed contained only four bays, coefficients obtained from the charts are in satisfactory agreement with those obtained by recurrence-formula solution and experiment.

RÉSUMÉ

Design charts are presented which are based on the solution of the finite-difference equation obtained in NACA Technical Note No. 1219. These charts permit the rapid determination of the following stresses and loads in circular cylinders loaded in the plane of one reinforcing ring:

(1) The shear flows in the sheet of the bays adjacent to the loaded ring

(2) The direct stresses in the effective skin at the loaded ring and at the two rings adjacent to this ring

(3) The moments, shears, and axial forces in the loaded ring and the two adjacent rings

For cylinders loaded at more than one ring or at several positions on the same ring, the total stresses can be obtained by superposition of those stresses determined from consideration of the cylinder for each individual load.

Langley Memorial Aeronautical Laboratory
National Advisory Committee for Aeronautics
Langley Field, Va., March 25, 1947

APPENDIX

NUMERICAL EXAMPLES

Cantilevered cylinder.- In order to illustrate the procedure used in the application of the charts to cantilevered cylinders, cylinder 2 of reference 4 is considered in this appendix. As indicated in the sketch of figure 48, the cylinder has four bays and is radially loaded at the middle reinforcing ring. The following properties of the cylinder are obtained from table 1 of reference 4:

R, in.	15
L, in.	15
t, in.	0.0320
I, in.^{4}	0.04001

Since the cylinder has no longitudinal reinforcements, $t' = t = 0.0320$ in. In reference 4 Young's modulus is taken as 10.6×10^3 ksi and the shear modulus as 4.00×10^3 ksi. Consequently,

$$A = \frac{15^6 \times 0.0320}{0.04001 \times 15^3} = 2700$$

and

$$\frac{A}{B} = \frac{4.00 \times 10^3 \times 0.032 \times 15^4}{10.6 \times 10^3 \times 0.04001 \times 15} = 1020$$

The values of A and A/B from the chart that are nearest to the computed values are

$$A = 2 \times 10^4$$

and

$$\frac{A}{B} = 10^3$$

The coefficients for loads and stresses that correspond to a radial load on the cylinder, therefore, are obtained from the curves corresponding to $\frac{A}{B} = 10^3$ in figures 18 to 22. The coefficients can be converted to loads and stresses with the aid of the formulas given in the charts and summarized in table 1. The coefficients for bending moments in the rings and shear flows in the sheet for this example are plotted in figures 48 and 49 where coefficients determined by other methods of analysis and by experiment are also plotted for comparison.

Simply supported cylinder.- If the beam analyzed in the previous problem is now considered simply supported at the end rings and radially loaded at the middle ring (see sketch in fig. 50), the elementary shear flow consistent with this method of support must be computed, and the correction shear flow due to the distortion of the cylinder can be determined from figure 21 $\left(A = 2 \times 10^4 \right.$ and $\left. \frac{A}{B} = 10^3\right)$. As mentioned in the section of the present paper entitled "APPLICATION OF DESIGN CHARTS," the coefficients for ring stresses and loads can be obtained directly from the charts (figs. 18 to 20). The elementary shear flow in bay 0 is

$$q_R = -\frac{P}{2\pi R} \sin \phi$$

A curve for shear-flow coefficients corresponding to this standard solution is given in figure 50. The correction shear-flow coefficients are determined from figure 21 by subtraction of the coefficients given by the curve for $\frac{A}{B} = 0$ from those given by the curve for $\frac{A}{B} = 10^3$. These corrections are plotted in figure 50. Addition of the elementary and correction-coefficient curves yields the curve for the total shear-flow coefficient, which is also shown in figure 50. Because of the symmetry of loading, the shear-flow coefficients for bay -1 are the negative of the corresponding coefficients for bay 0.

REFERENCES

1. Duberg, John E., and Kempner, Joseph: Stress Analysis by Recurrence Formula of Reinforced Circular Cylinders under Lateral Loads. NACA TN No. 1219, 1947.

2. Wignot, J. E., Combs, Henry, and Ensrud, A. F.: Analysis of Circular Shell-Supported Frames. NACA TN No. 929, 1944.

3. Hoff, N. J.: Stresses in a Reinforced Monocoque Cylinder under Concentrated Symmetric Transverse Loads. Jour. Appl. Mech., vol. 11, no. 4, Dec. 1944, pp. A-235 - A-239.

4. Kuhn, Paul, Duberg, John E., and Griffith, George E.: The Effect of Concentrated Loads on Flexible Rings in Circular Shells. NACA ARR No. L5H23, 1945.

5. Wise, Joseph A.: Analysis of Circular Rings for Monocoque Fuselages. Jour. Aero. Sci., vol. 6, no. 11, Sept. 1939, pp. 460-463.

TABLE I.- FORMULAS FOR LOADS AND STRESSES

[Sign convention is shown in figure 2]

Quantity to be calculated	Radial load, P	Tangential load, T	Moment load, M
Bending moment	$M_\phi = C_{mr}PR = M_{-\phi}$	$M_\phi = C_{mt}TR = -M_{-\phi}$	$M_\phi = C_{mm}M = -M_{-\phi}$
Axial force	$H_\phi = C_{ar}P = H_{-\phi}$	$H_\phi = C_{at}T = -H_{-\phi}$	$H_\phi = C_{am}\frac{M}{R} = -H_{-\phi}$
Shearing force	$V_\phi = C_{sr}P = -V_{-\phi}$	$V_\phi = C_{st}T = V_{-\phi}$	$V_\phi = C_{sm}\frac{M}{R} = V_{-\phi}$
Shear flow	$q_\phi = C_{qr}\frac{P}{R} = -q_{-\phi}$	$q_\phi = C_{qt}\frac{T}{R} = q_{-\phi}$	$q_\phi = C_{qm}\frac{M}{R^2} = q_{-\phi}$
Direct stress	$\sigma_\phi = C_{\sigma r}\frac{PL}{R^2t'} = \sigma_{-\phi}$	$\sigma_\phi = C_{\sigma t}\frac{TL}{R^2t'} = -\sigma_{-\phi}$	$\sigma_\phi = C_{\sigma m}\frac{ML}{R^3t'} = -\sigma_{-\phi}$

NATIONAL ADVISORY
COMMITTEE FOR AERONAUTICS

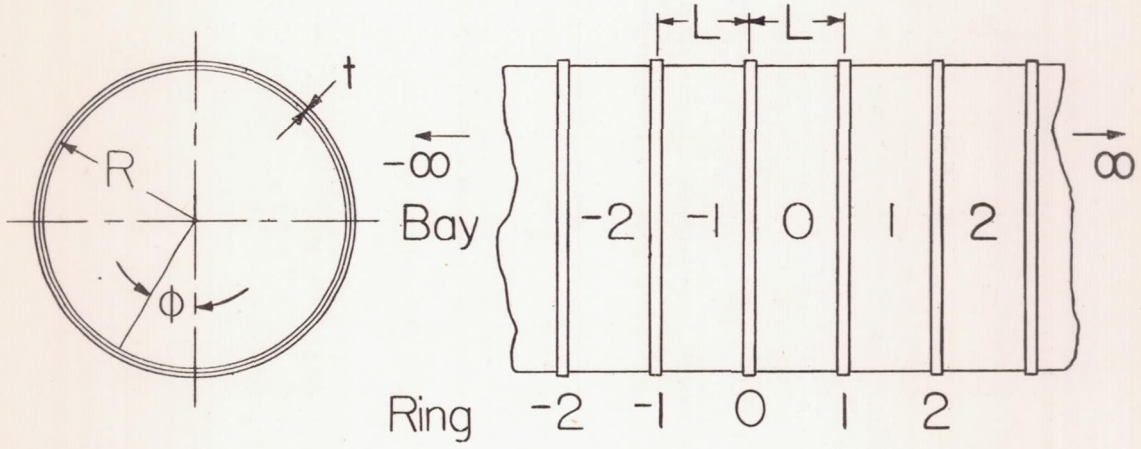

Figure 1.- Part of infinitely long cylinder.

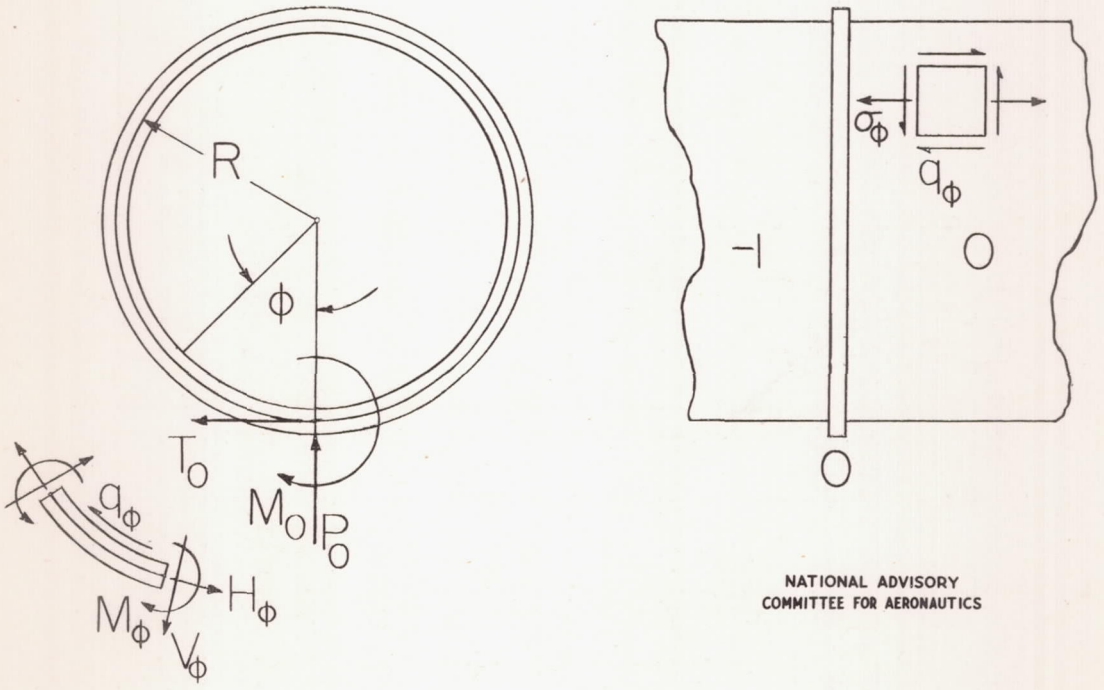

Figure 2.- Sign convention.

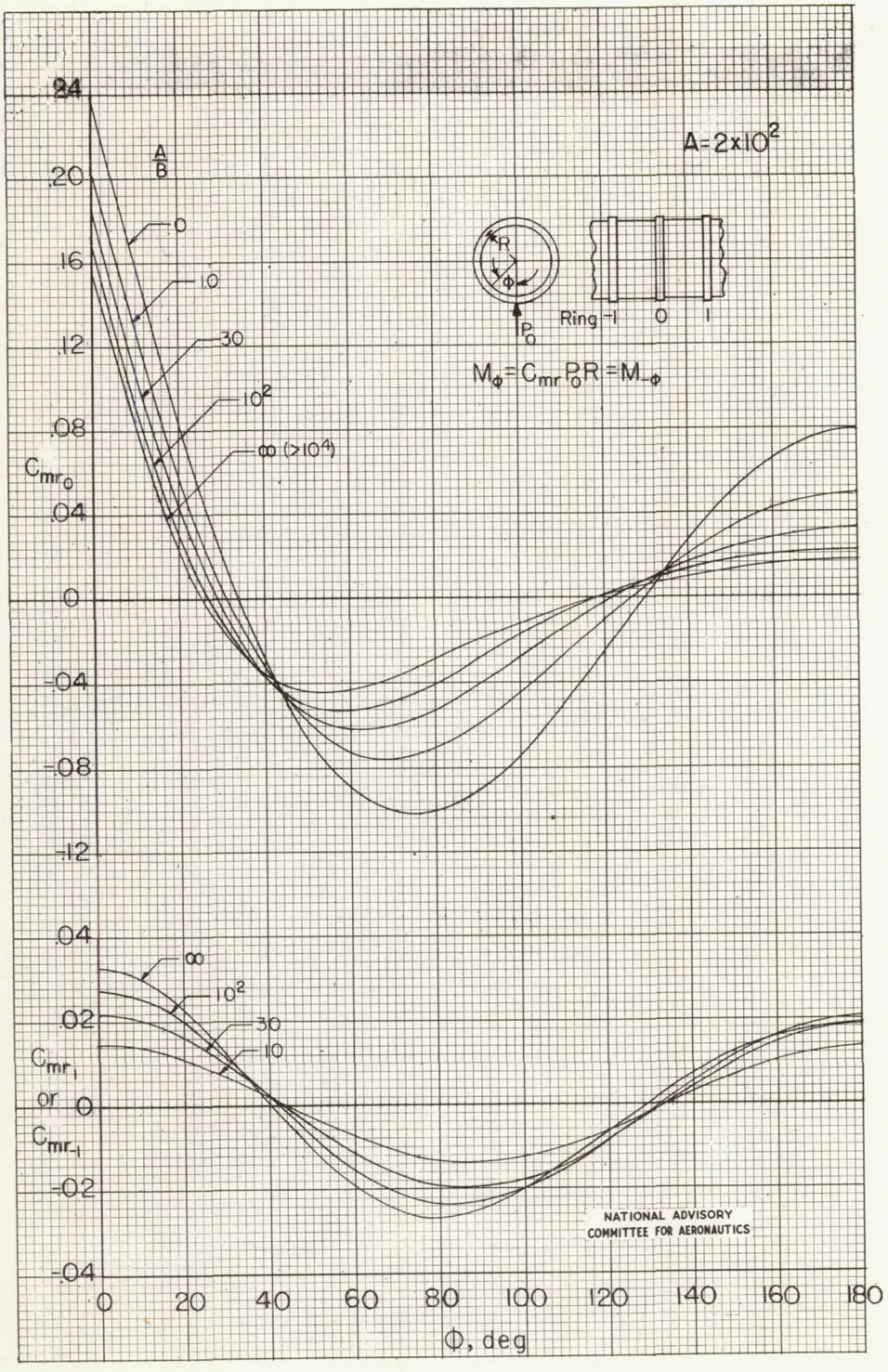

Figure 3.- Ring bending-moment coefficients for radial load. ($A = 2 \times 10^2$.)

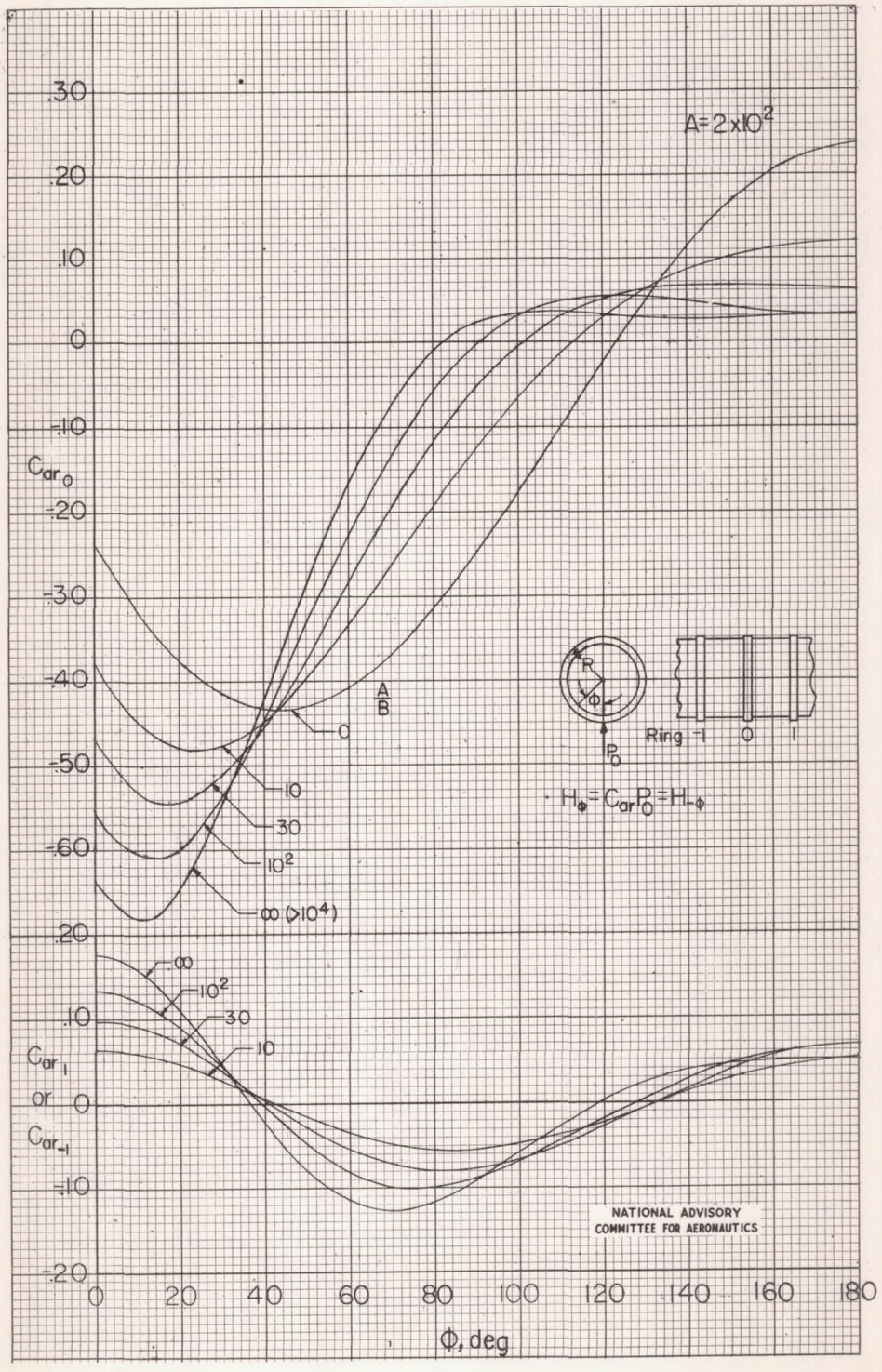

Figure 4.- Ring axial-load coefficients for radial load.
($A = 2 \times 10^2$.)

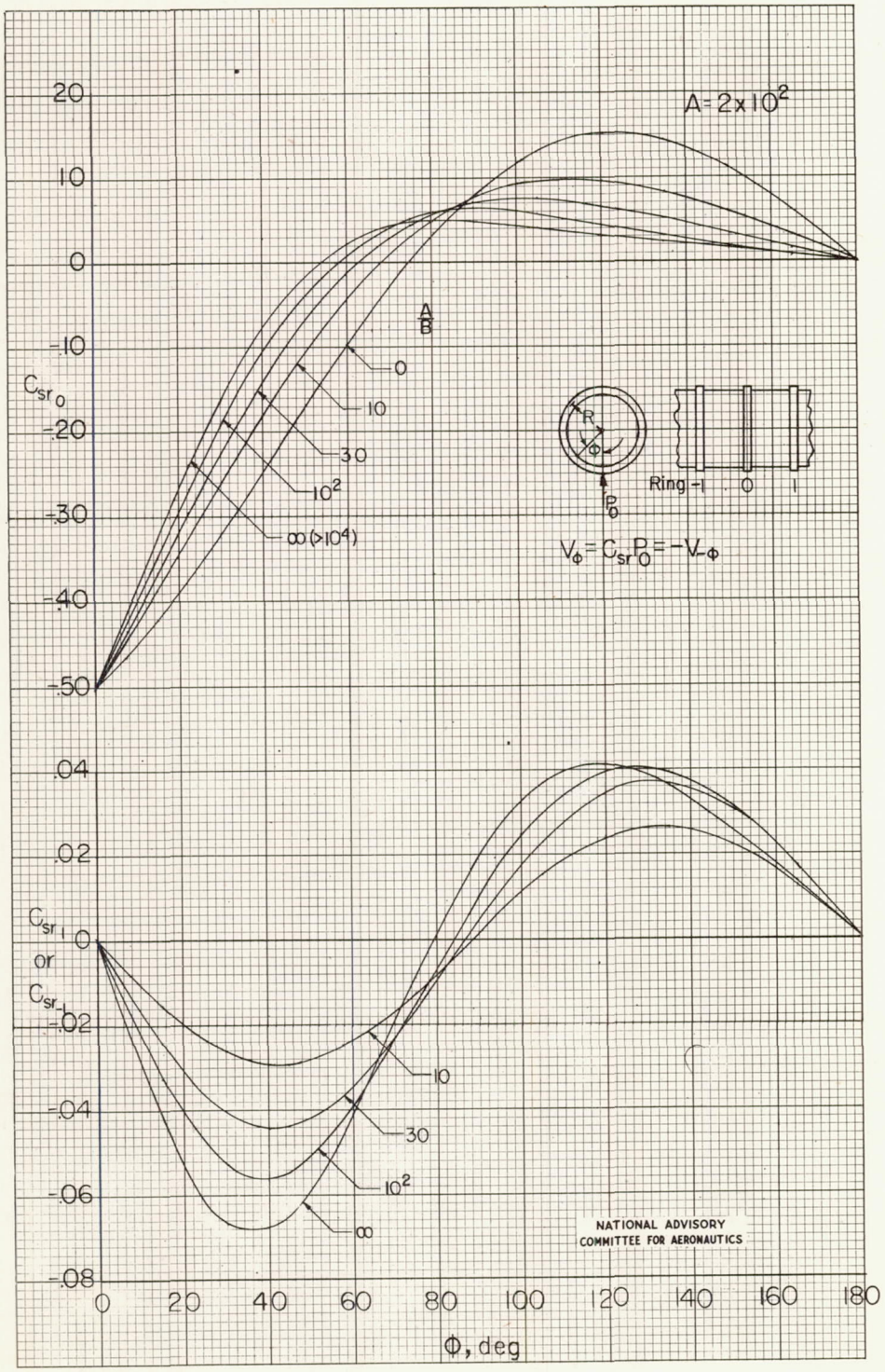

Figure 5.- Ring transverse-shear coefficients for radial load. ($A = 2 \times 10^2$.)

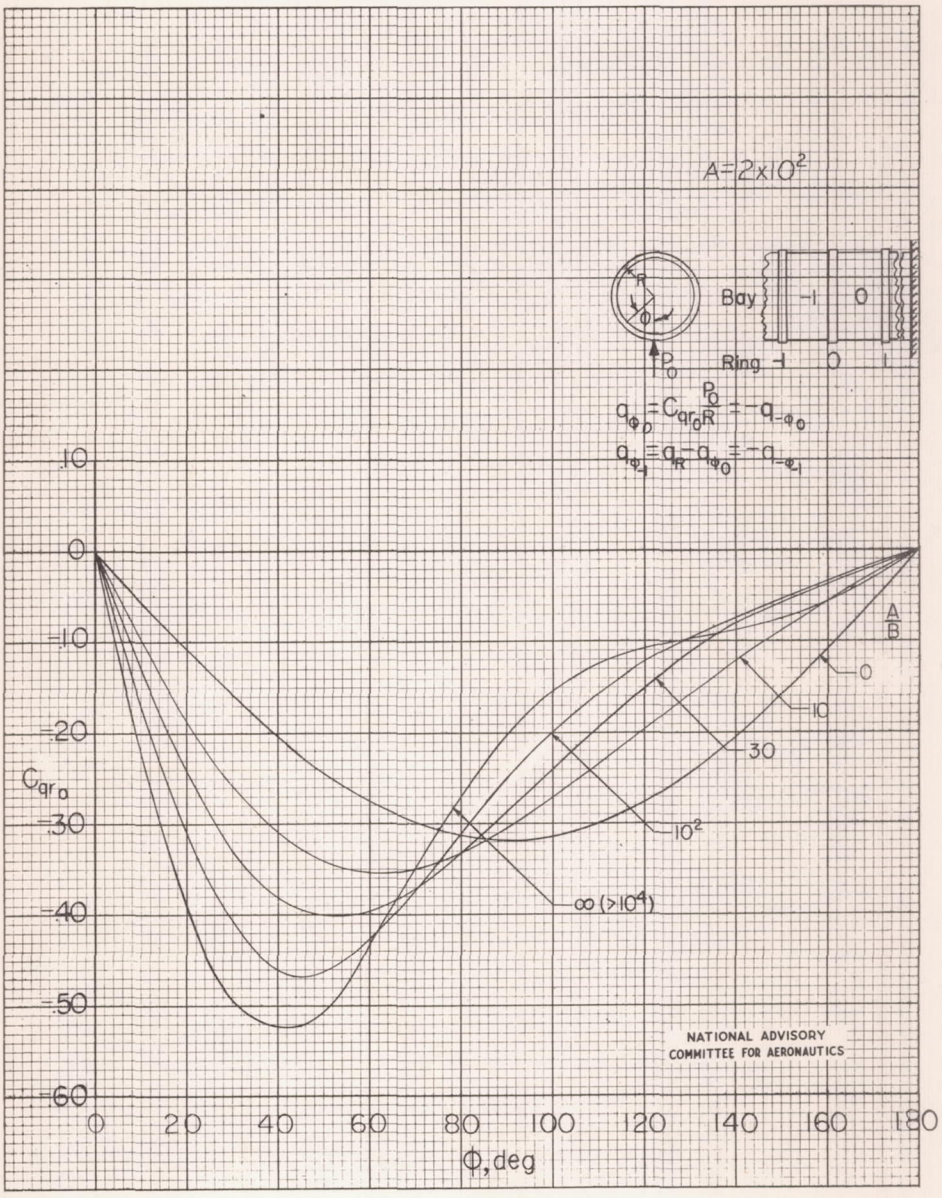

Figure 6.- Skin shear-flow coefficients for radial load.
($A = 2 \times 10^2$.)

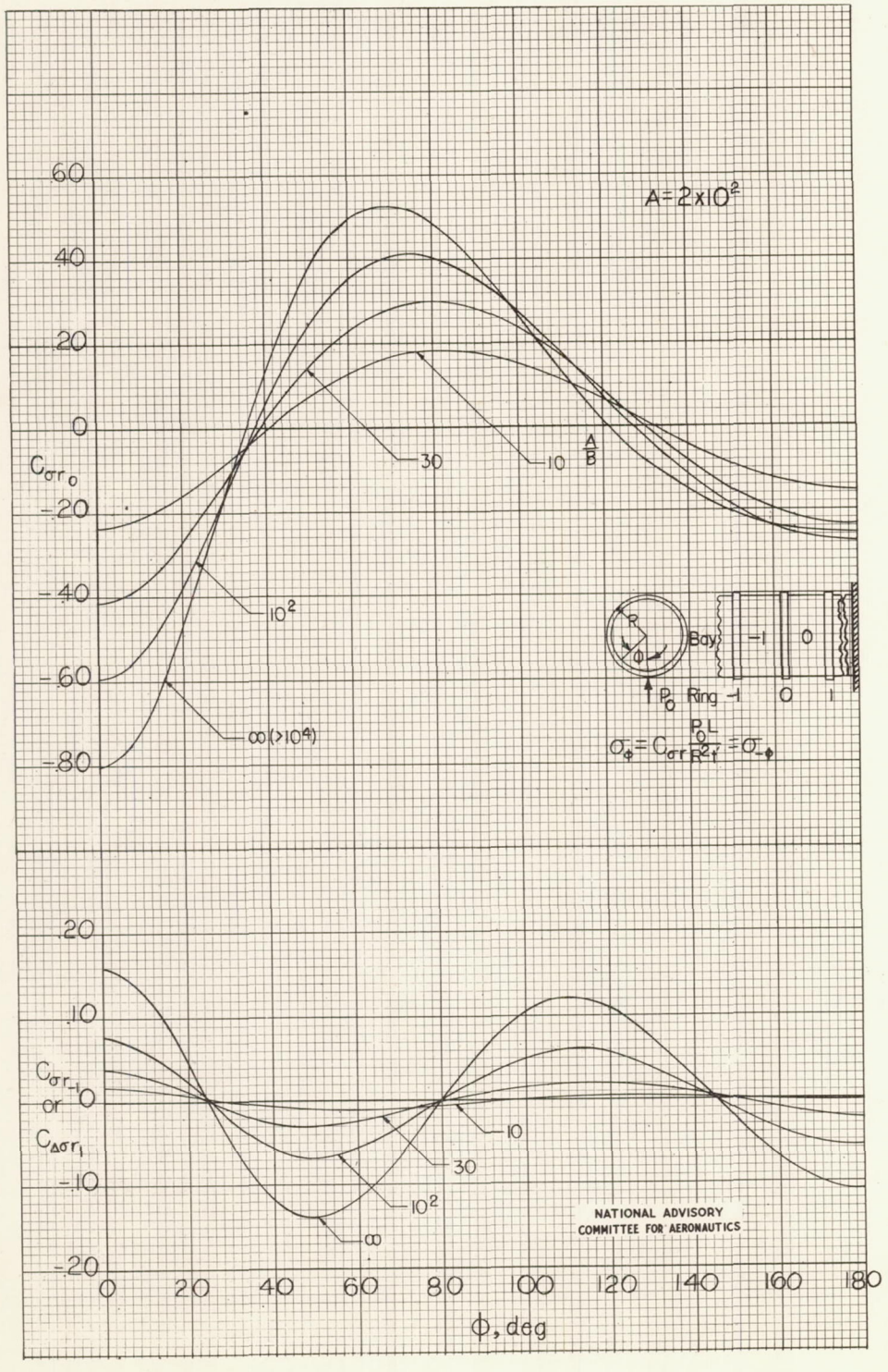

Figure 7.- Skin direct-stress coefficients at rings for radial load. ($A = 2 \times 10^2$.)

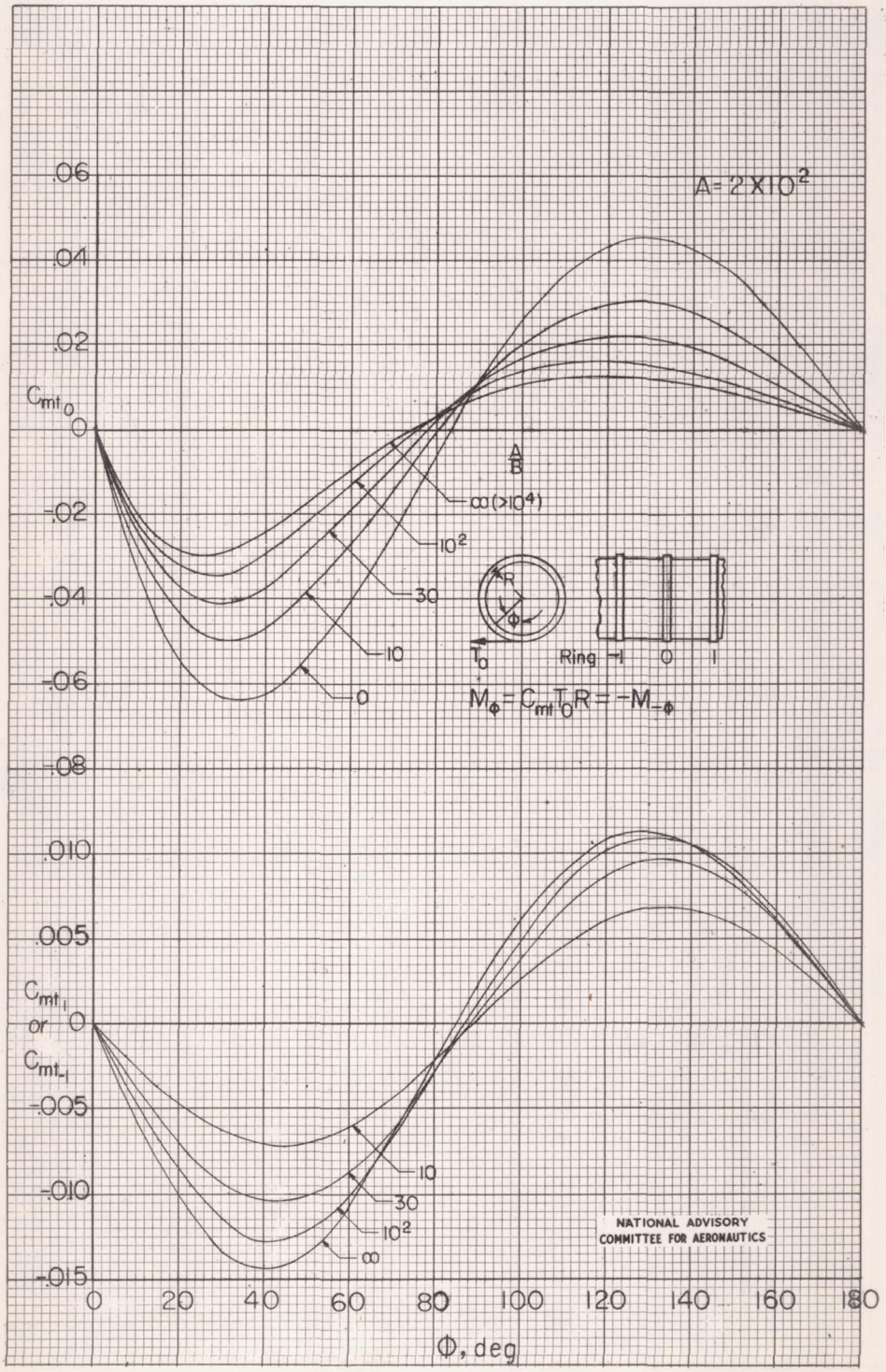

Figure 8.- Ring bending-moment coefficients for tangential load. ($A = 2 \times 10^2$.)

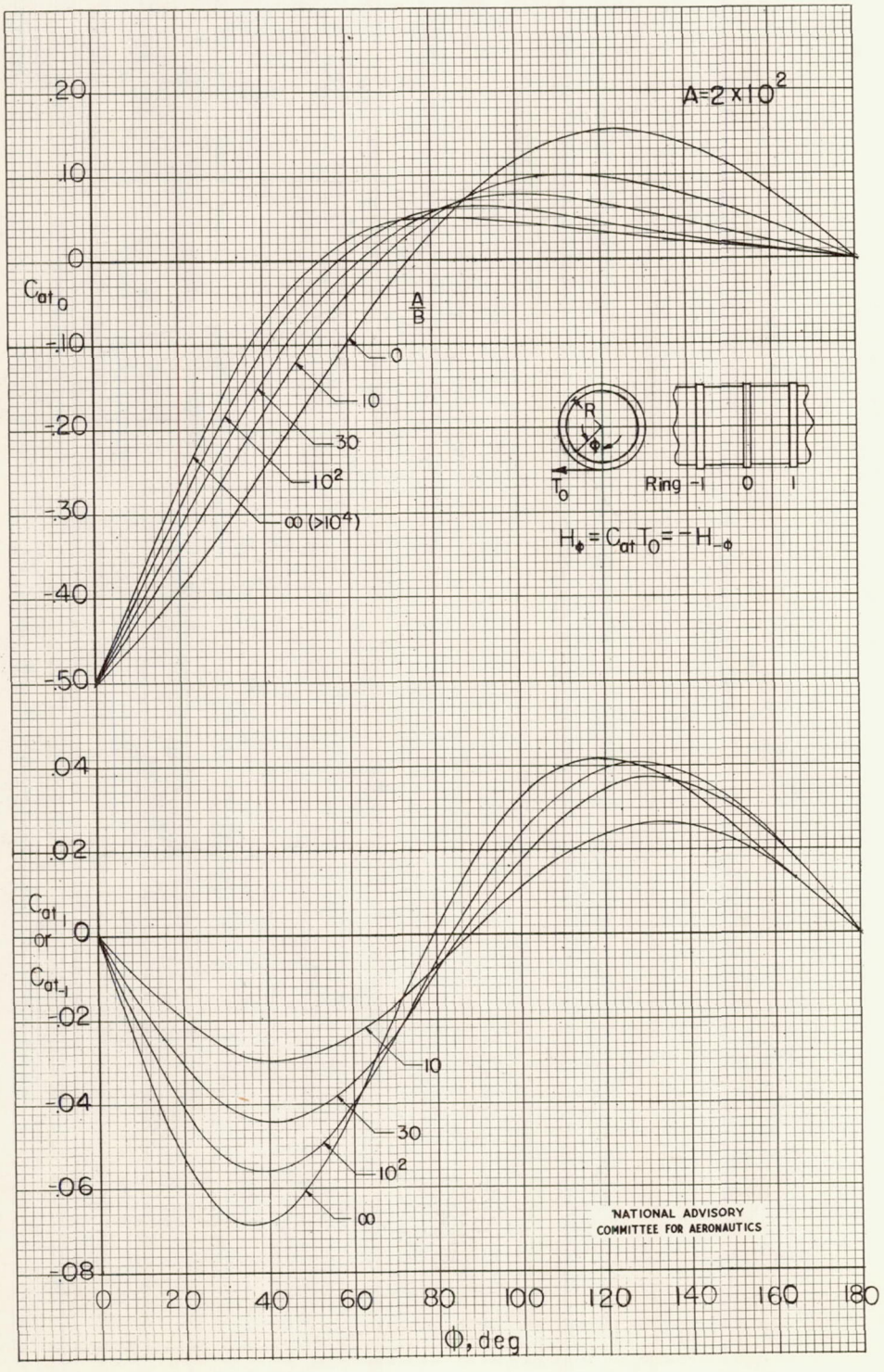

Figure 9.- Ring axial-load coefficients for tangential load.

($A = 2 \times 10^2$.)

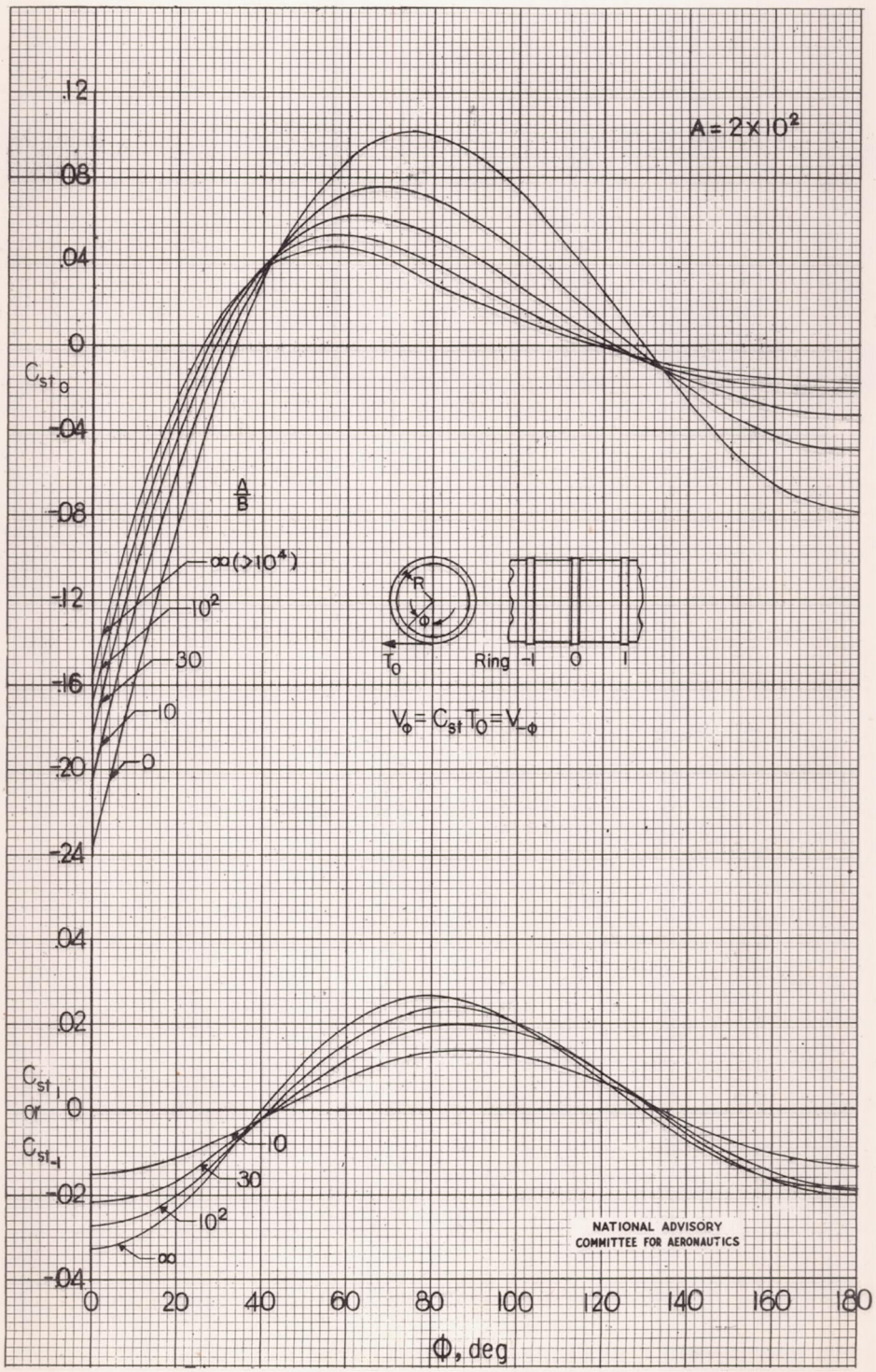

Figure 10.- Ring transverse-shear coefficients for tangential load. ($A = 2 \times 10^2$.)

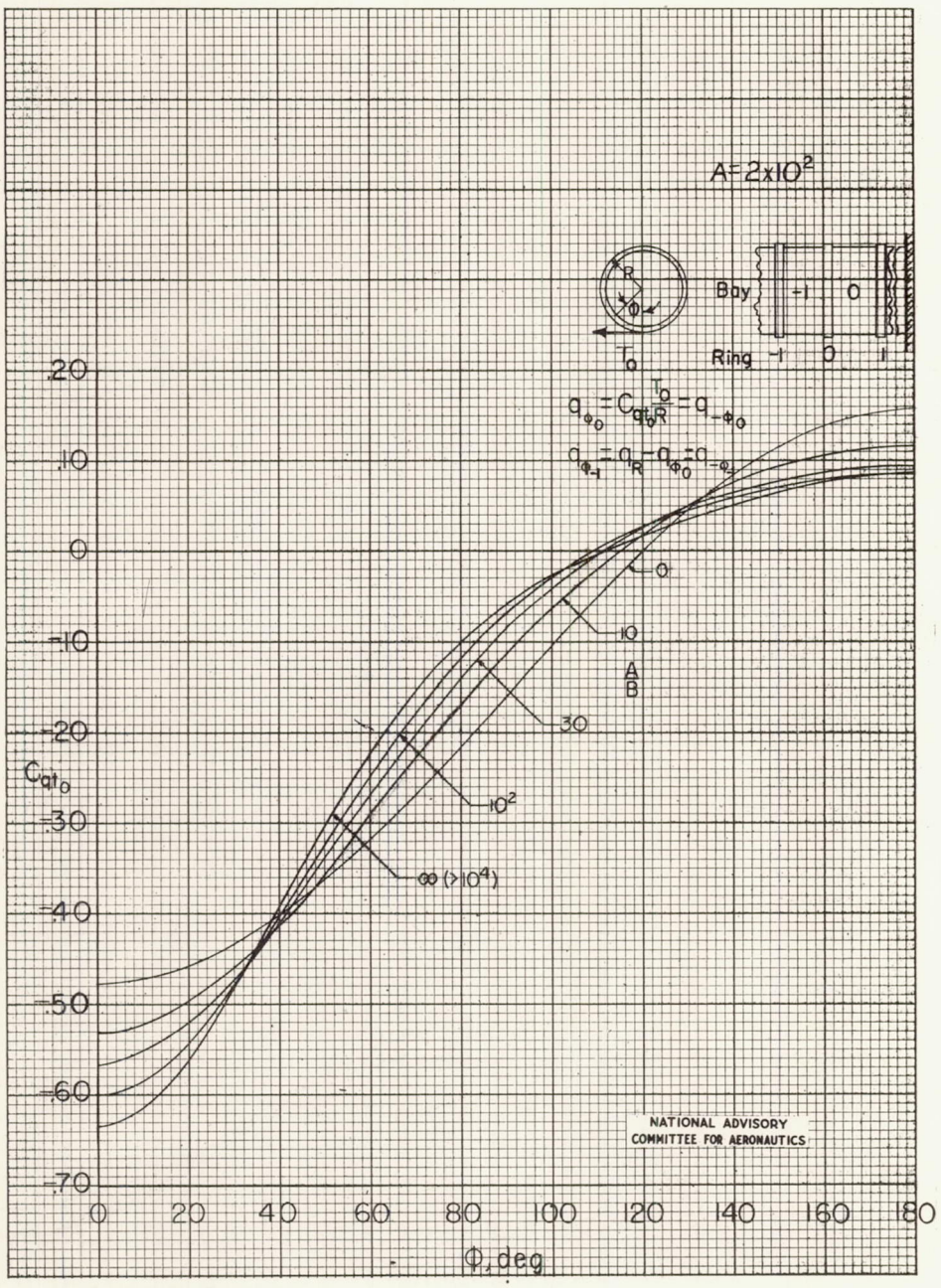

Figure 11.- Skin shear-flow coefficients for tangential load.
($A = 2 \times 10^2$.)

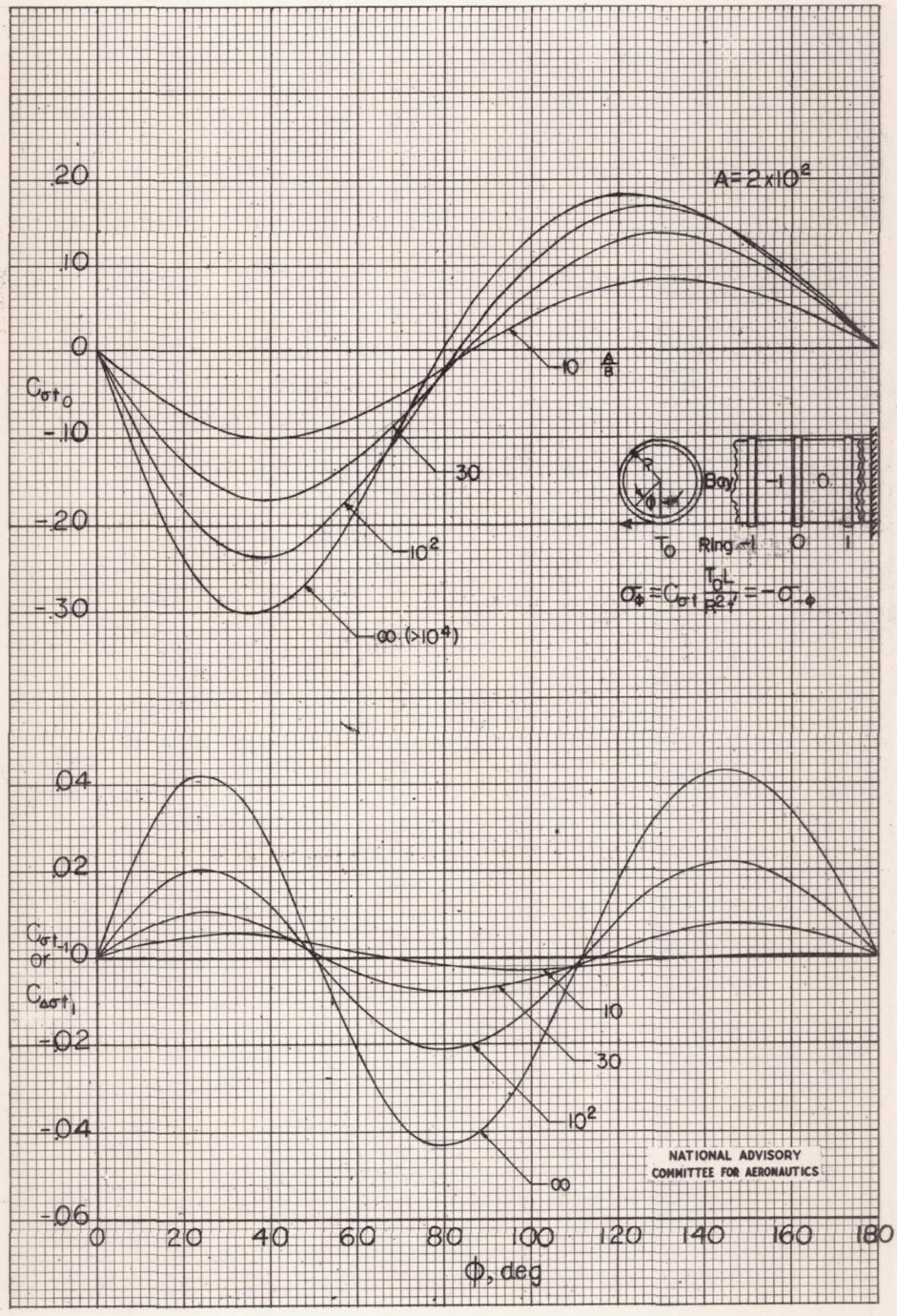

Figure 12.- Skin direct-stress coefficients at rings for tangential load. ($A = 2 \times 10^2$.)

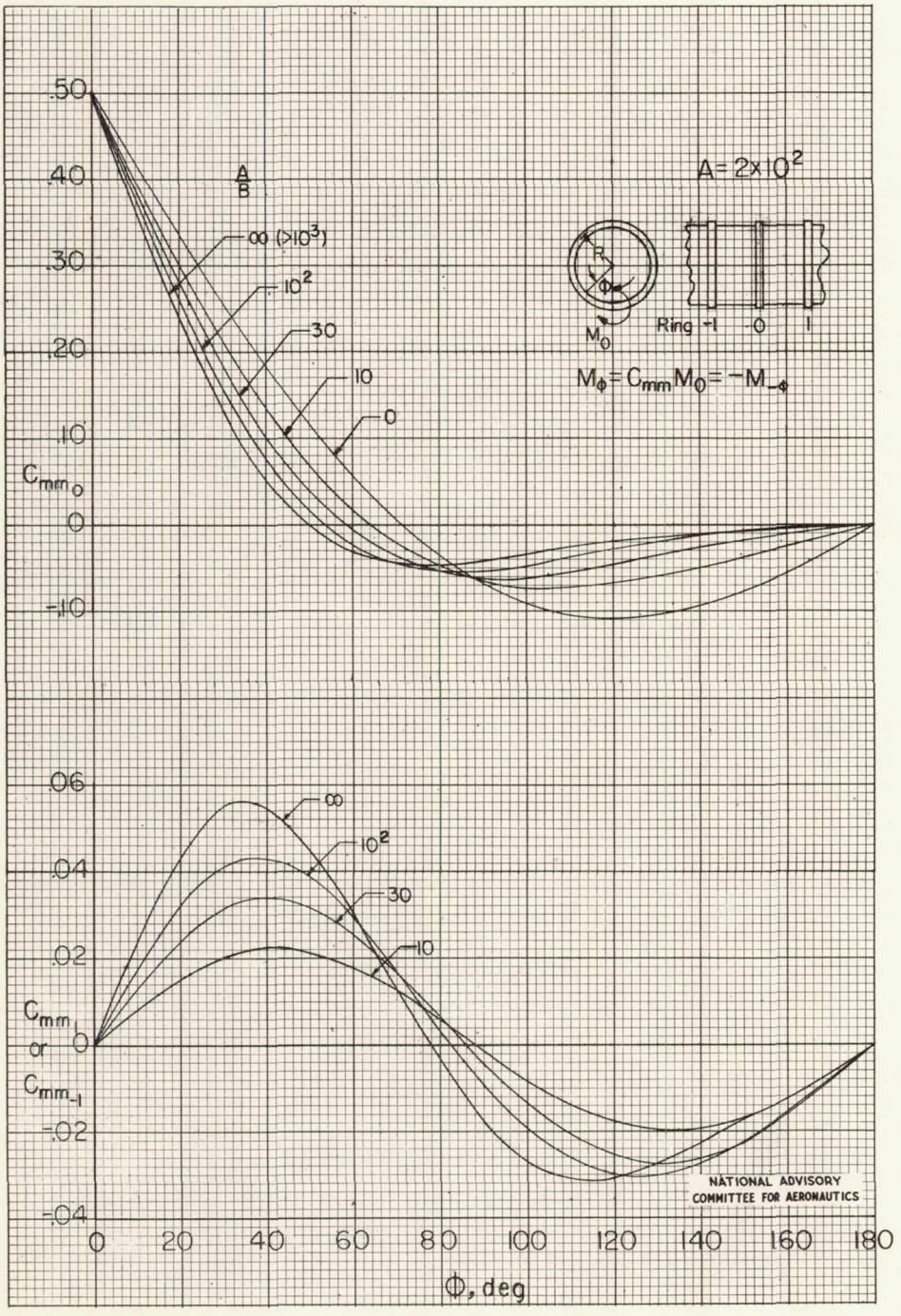

Figure 13.- Ring bending-moment coefficients for moment load. ($A = 2 \times 10^2$.)

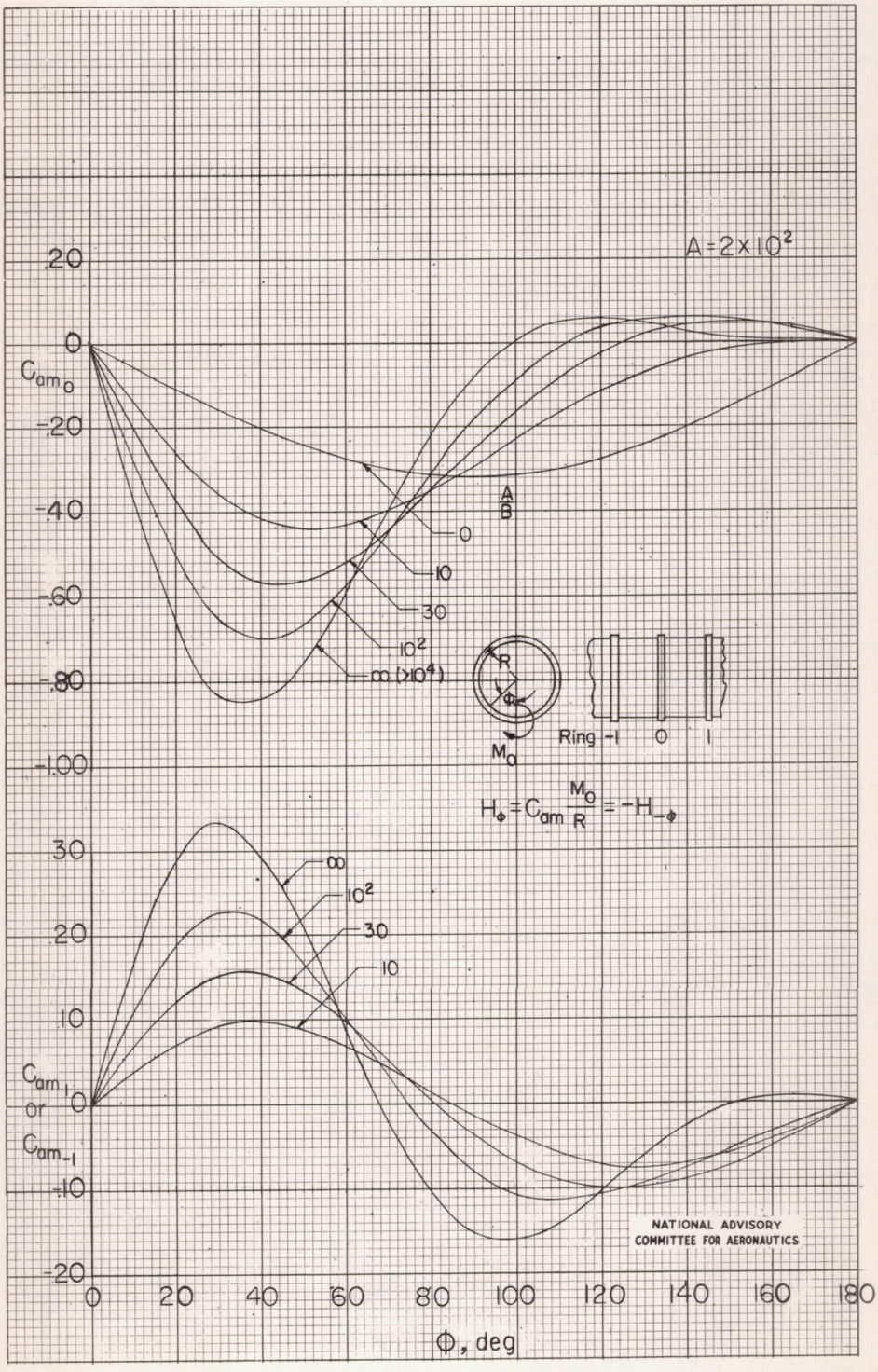

Figure 14.- Ring axial-load coefficients for moment load. ($A = 2 \times 10^2$.)

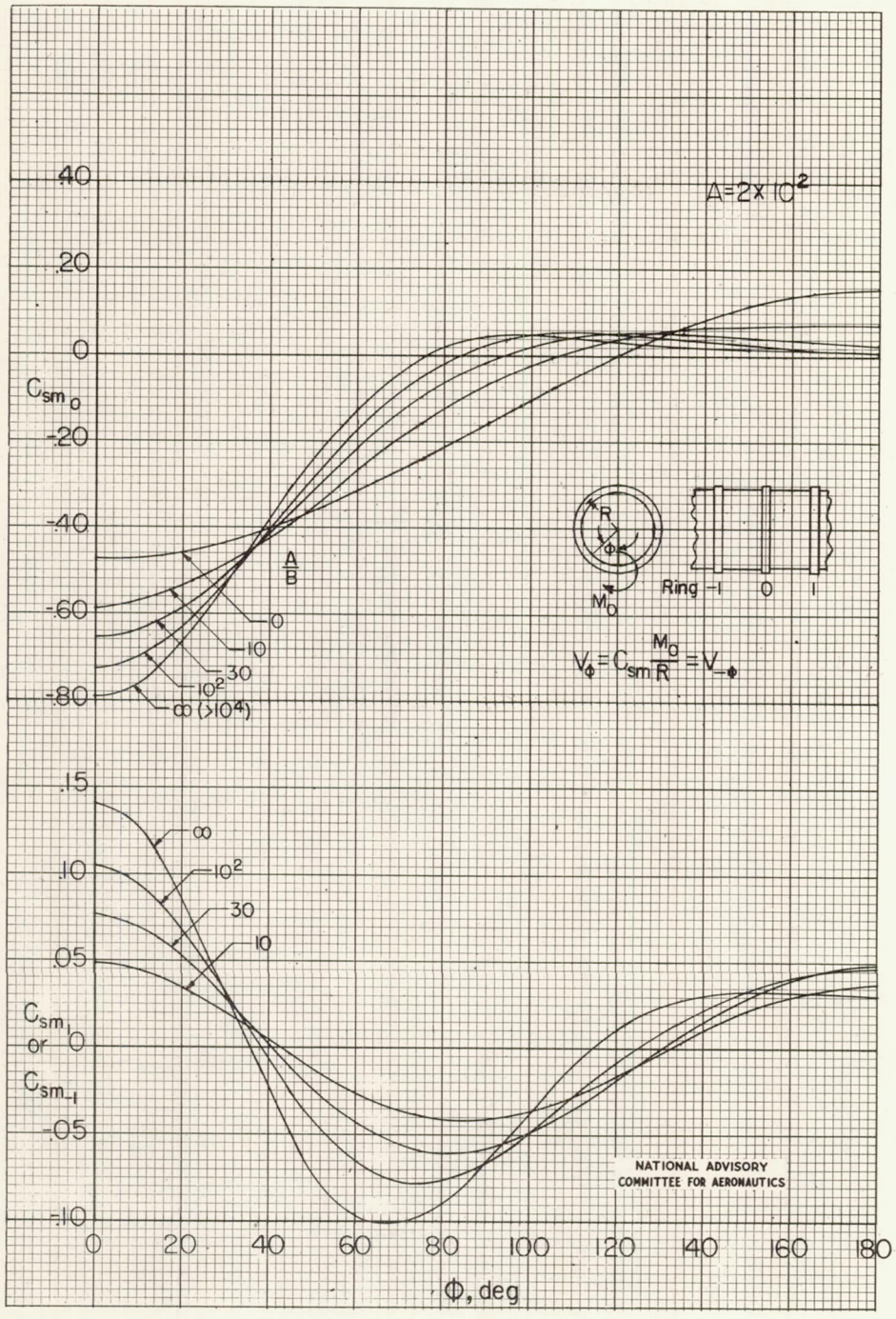

Figure 15.- Ring transverse-shear coefficients for moment load. ($A = 2 \times 10^2$.)

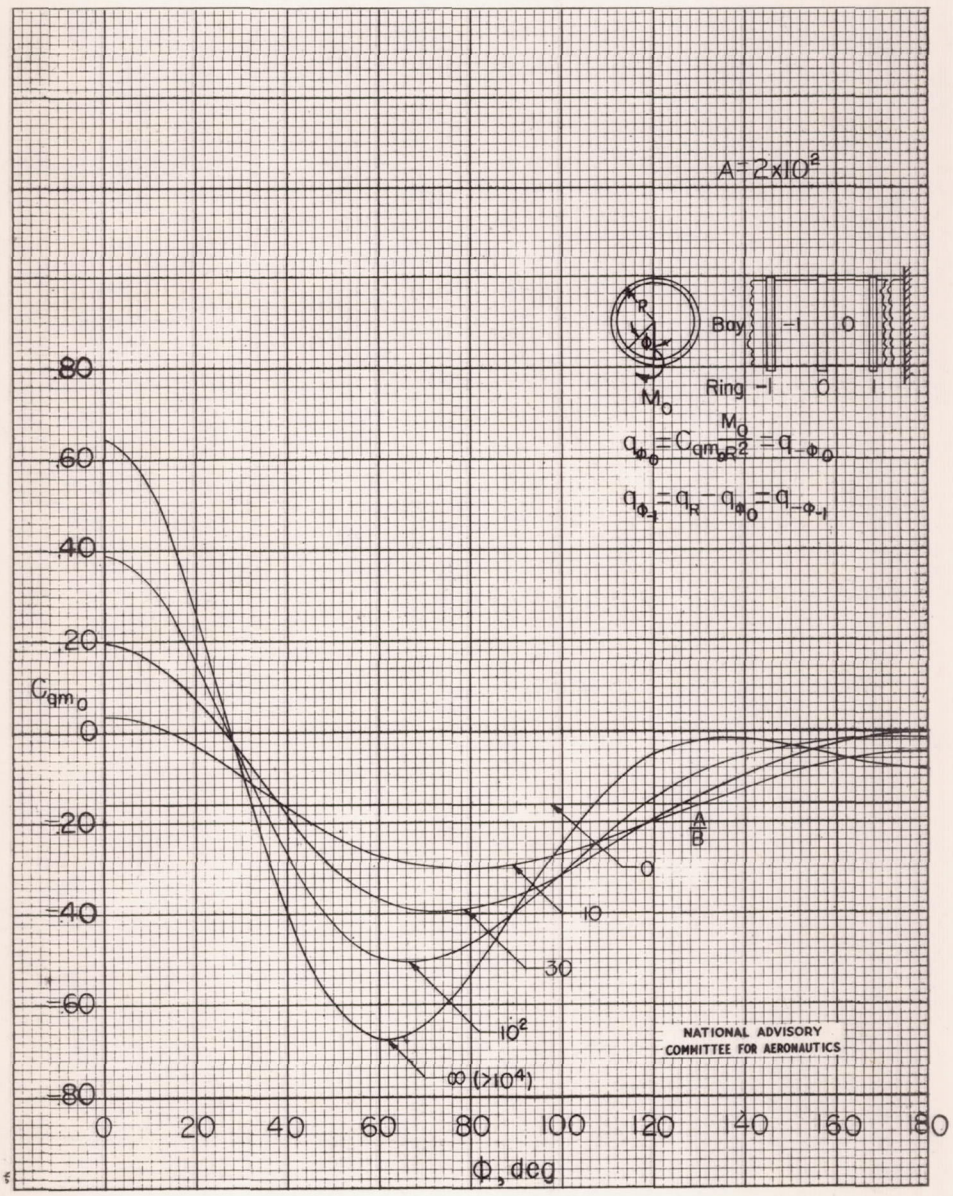

Figure 16.- Skin shear-flow coefficients for moment load. ($A = 2 \times 10^2$.)

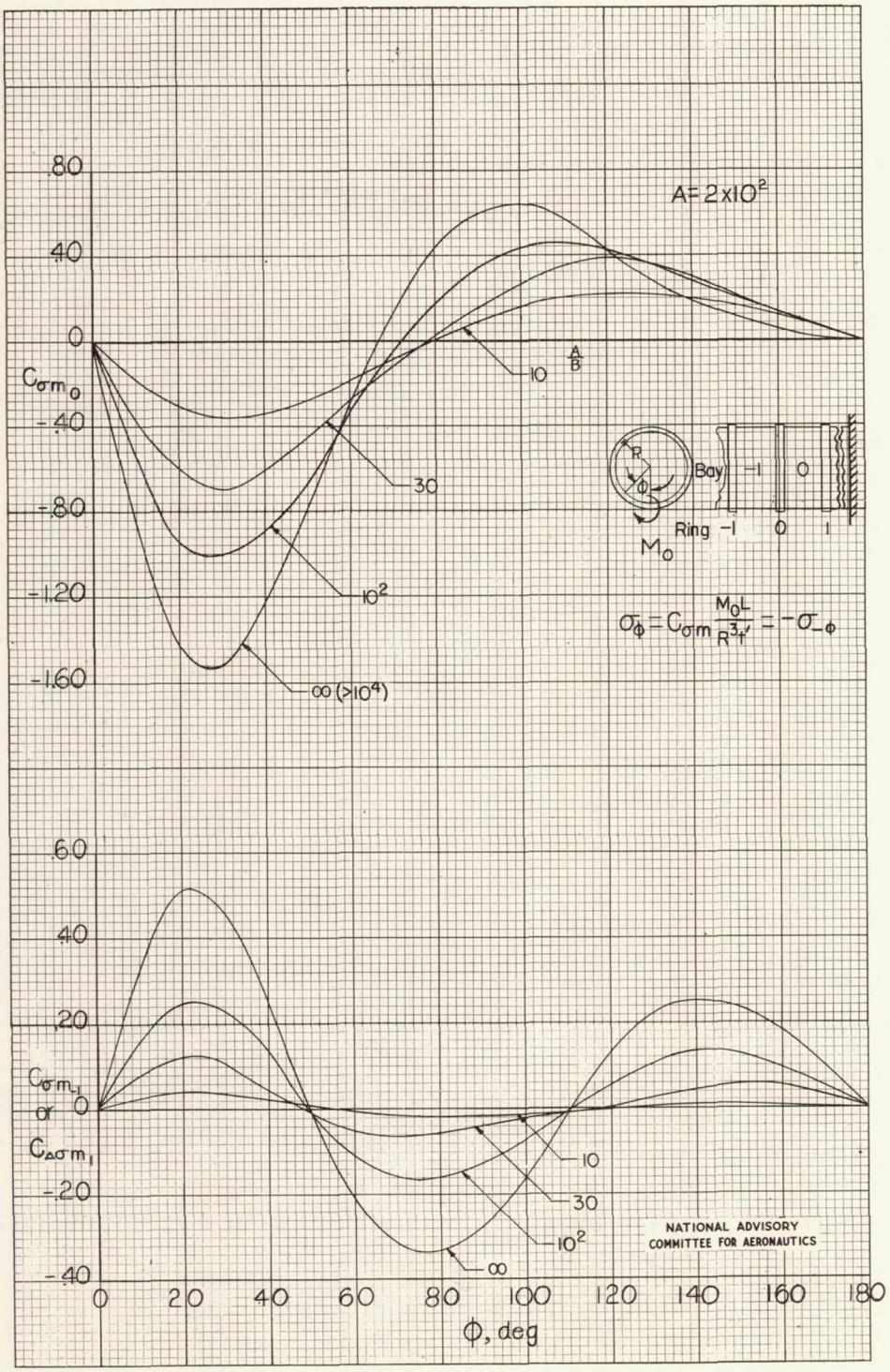

Figure 17.- Skin direct-stress coefficients at rings for moment load. ($A = 2 \times 10^2$.)

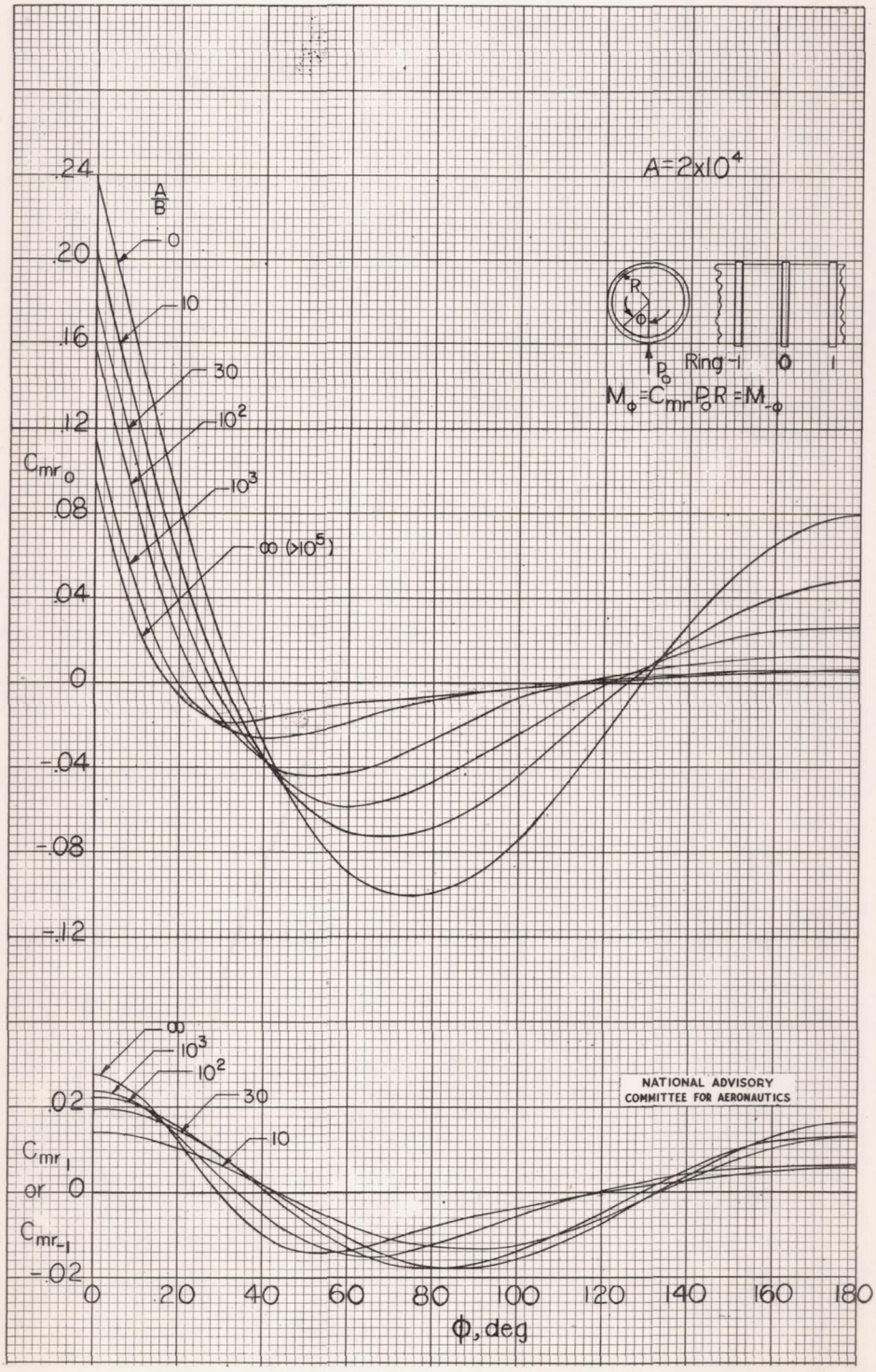

Figure 18.- Ring bending-moment coefficients for radial load. ($A = 2 \times 10^4$.)

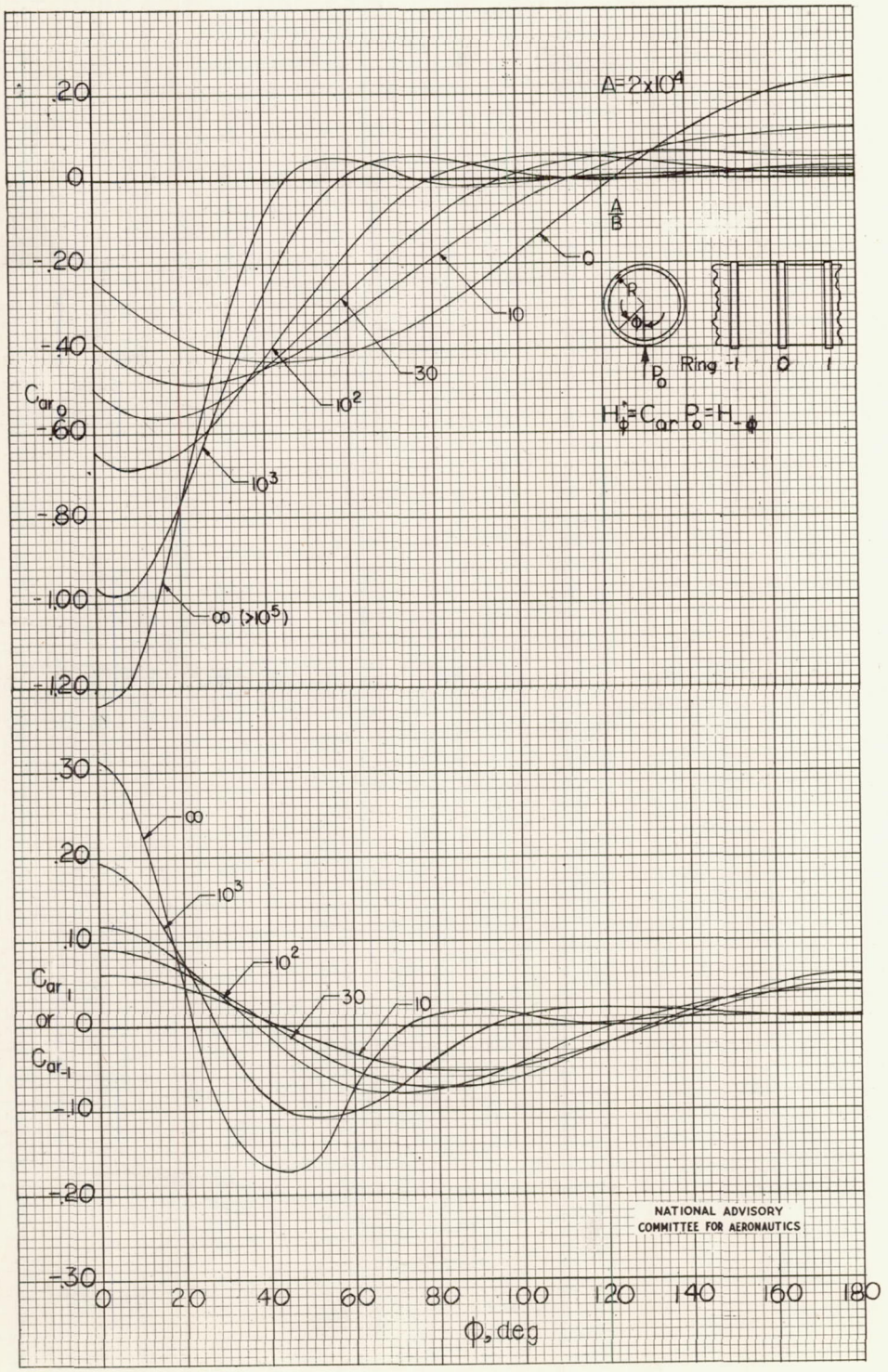

Figure 19.- Ring axial-load coefficients for radial load. ($A = 2 \times 10^4$.)

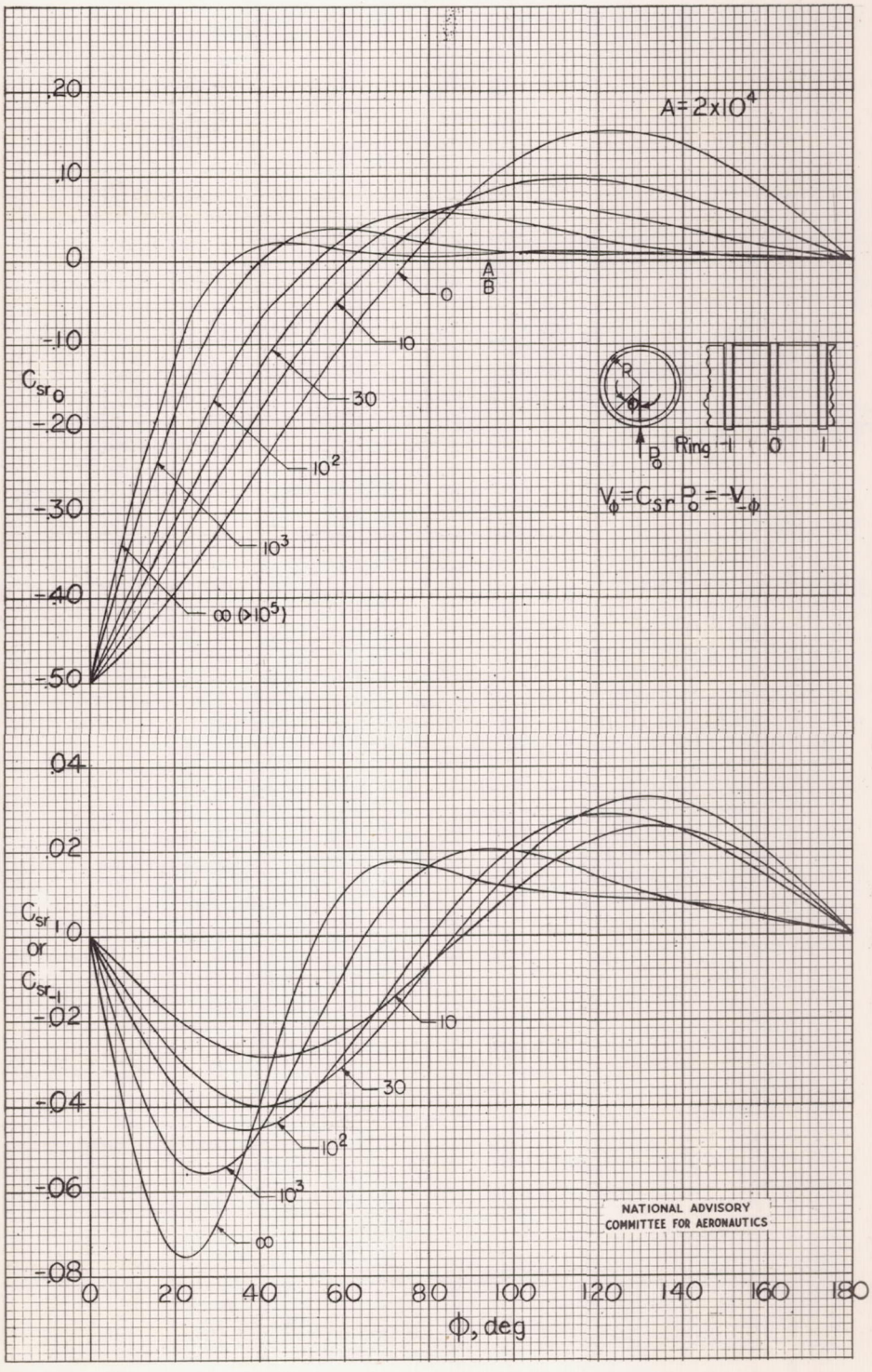

Figure 20.- Ring transverse-shear coefficients for radial load. ($A = 2 \times 10^4$.)

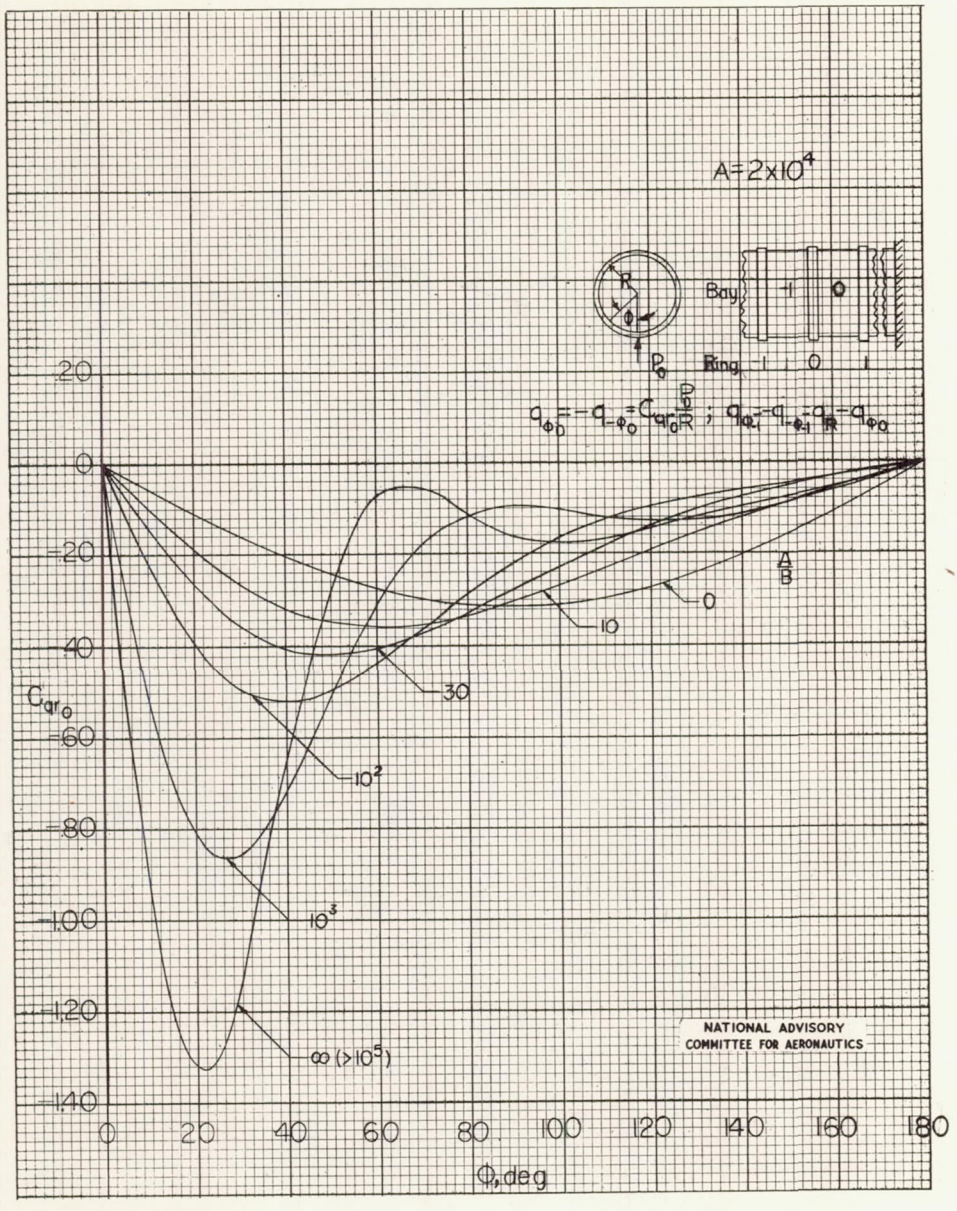

Figure 21.- Skin shear-flow coefficients for radial load.
($A = 2 \times 10^4$.)

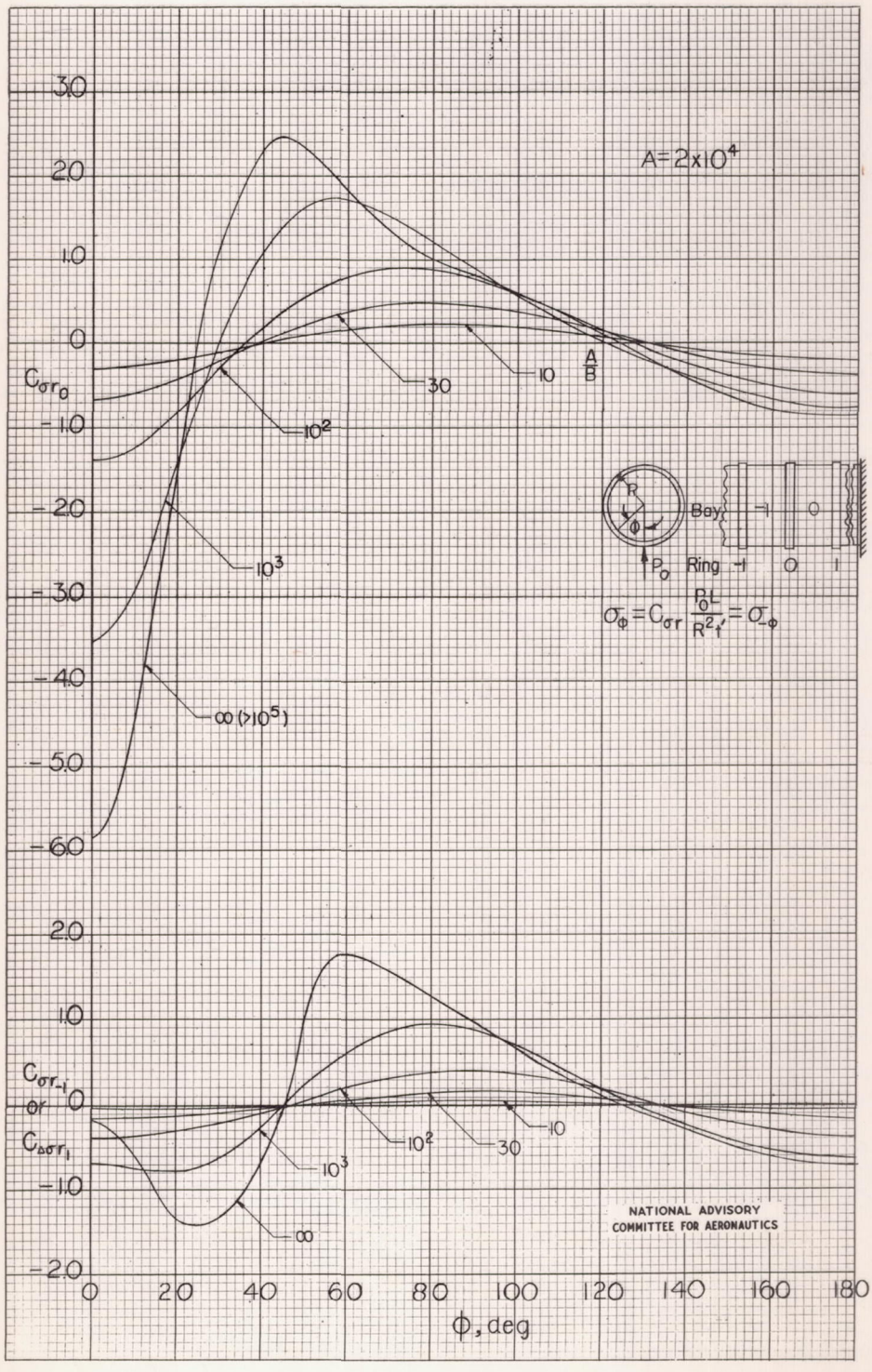

Figure 22.- Skin direct-stress coefficients at rings for radial load. ($A = 2 \times 10^4$.)

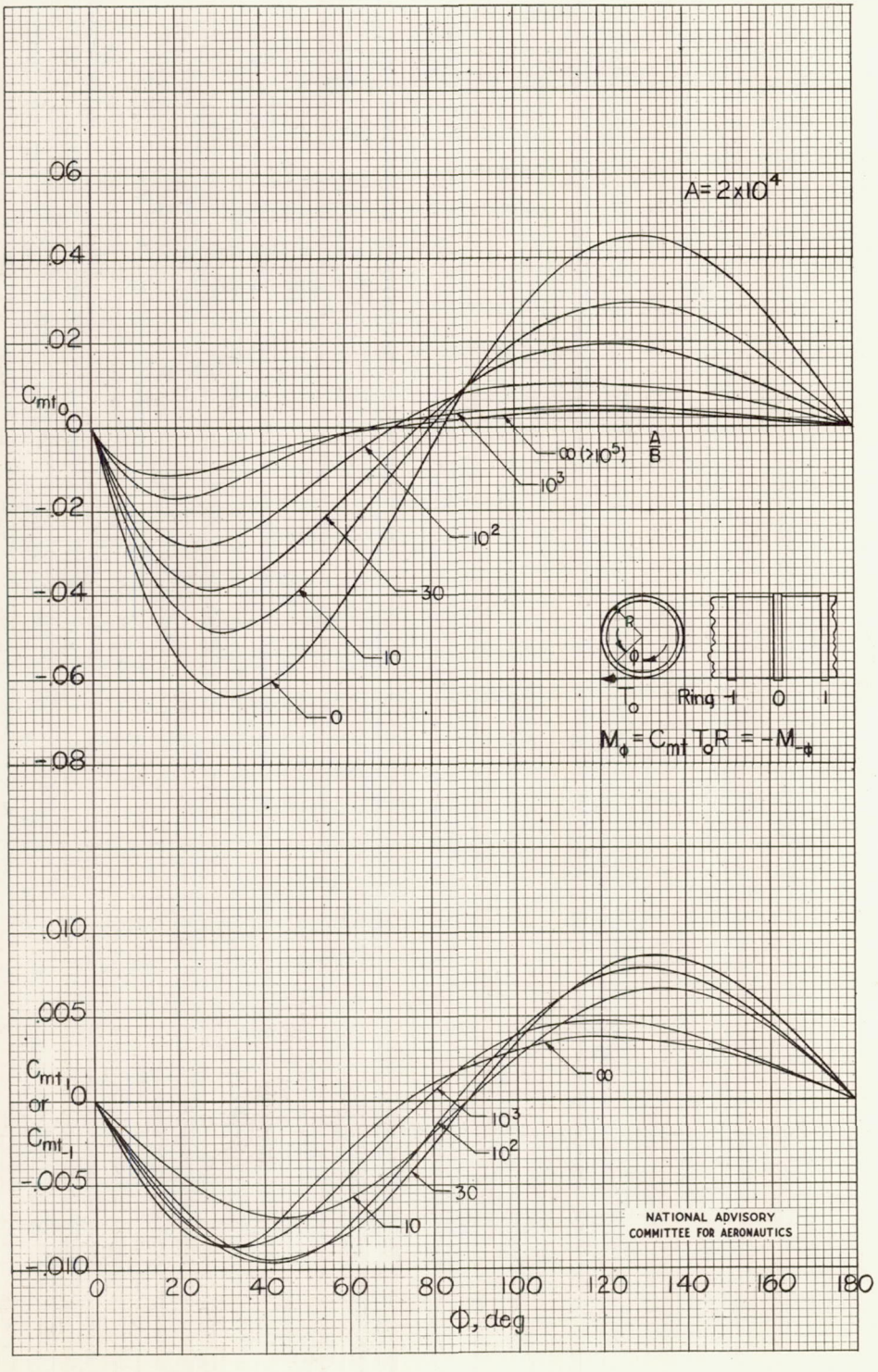

Figure 23.- Ring bending-moment coefficients for tangential load. ($A = 2 \times 10^4$.)

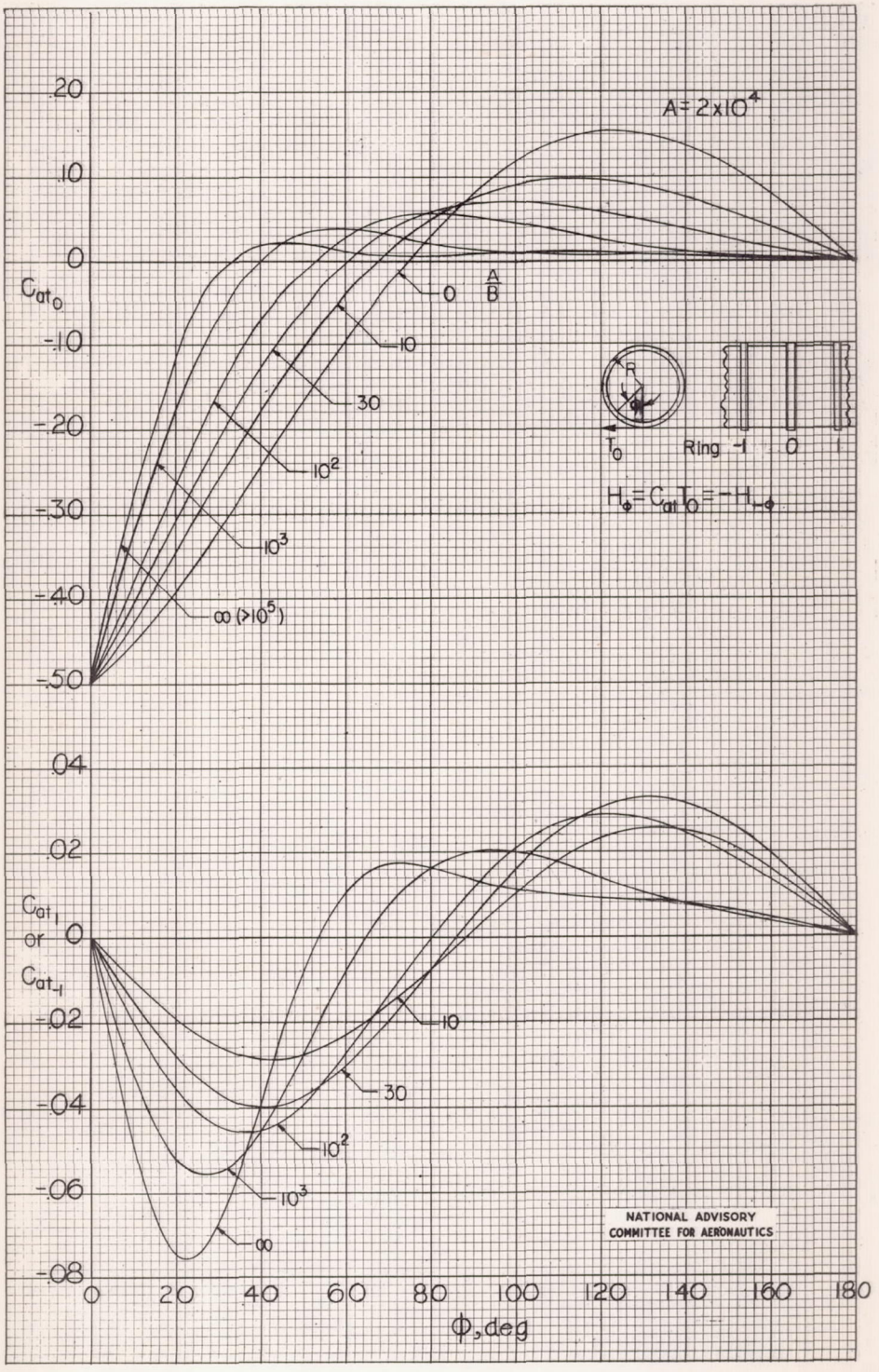

Figure 24.- Ring axial-load coefficients for tangential load. ($A = 2 \times 10^4$.)

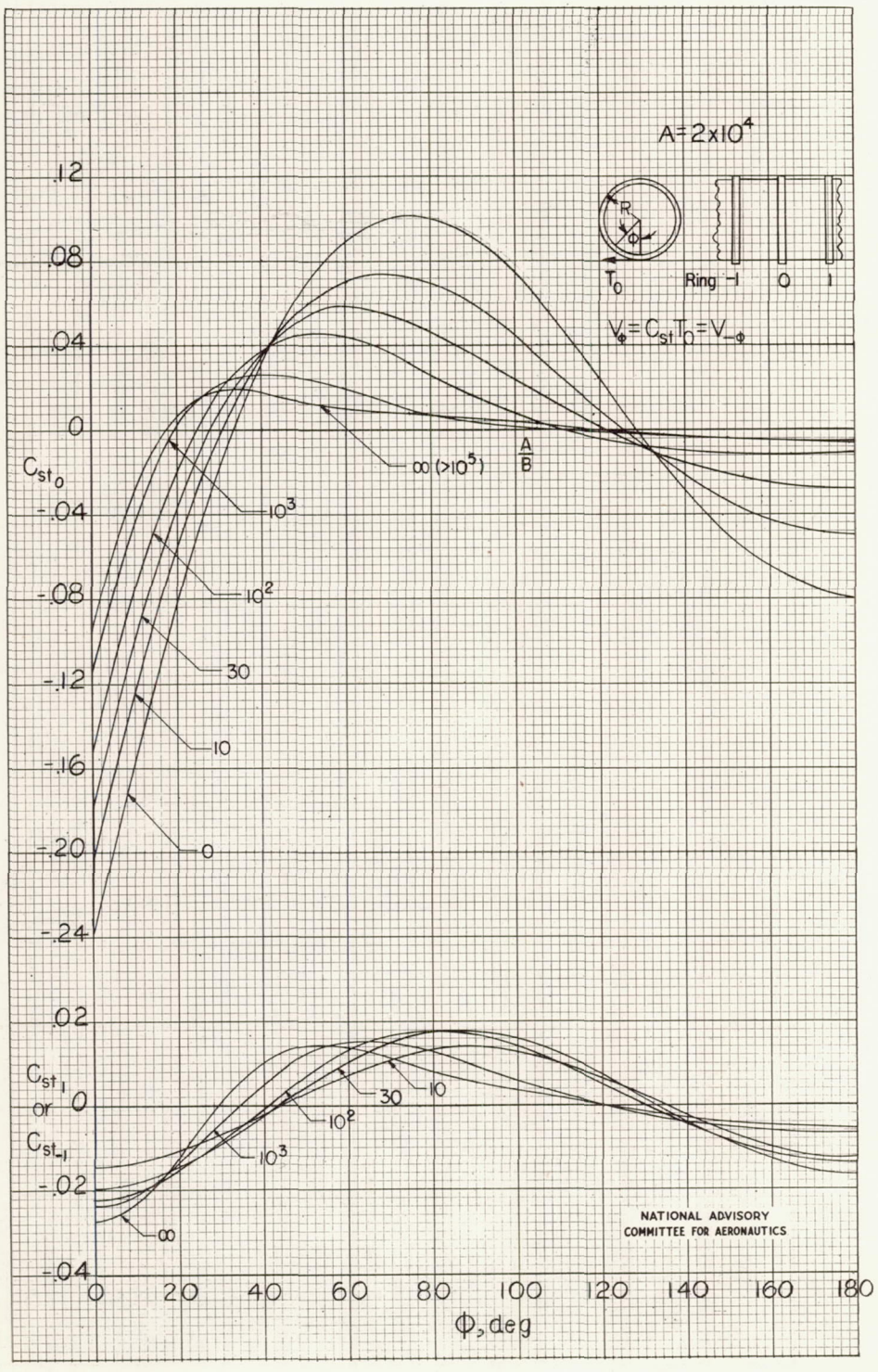

Figure 25.- Ring transverse-shear coefficients for tangential load. ($A = 2 \times 10^4$.)

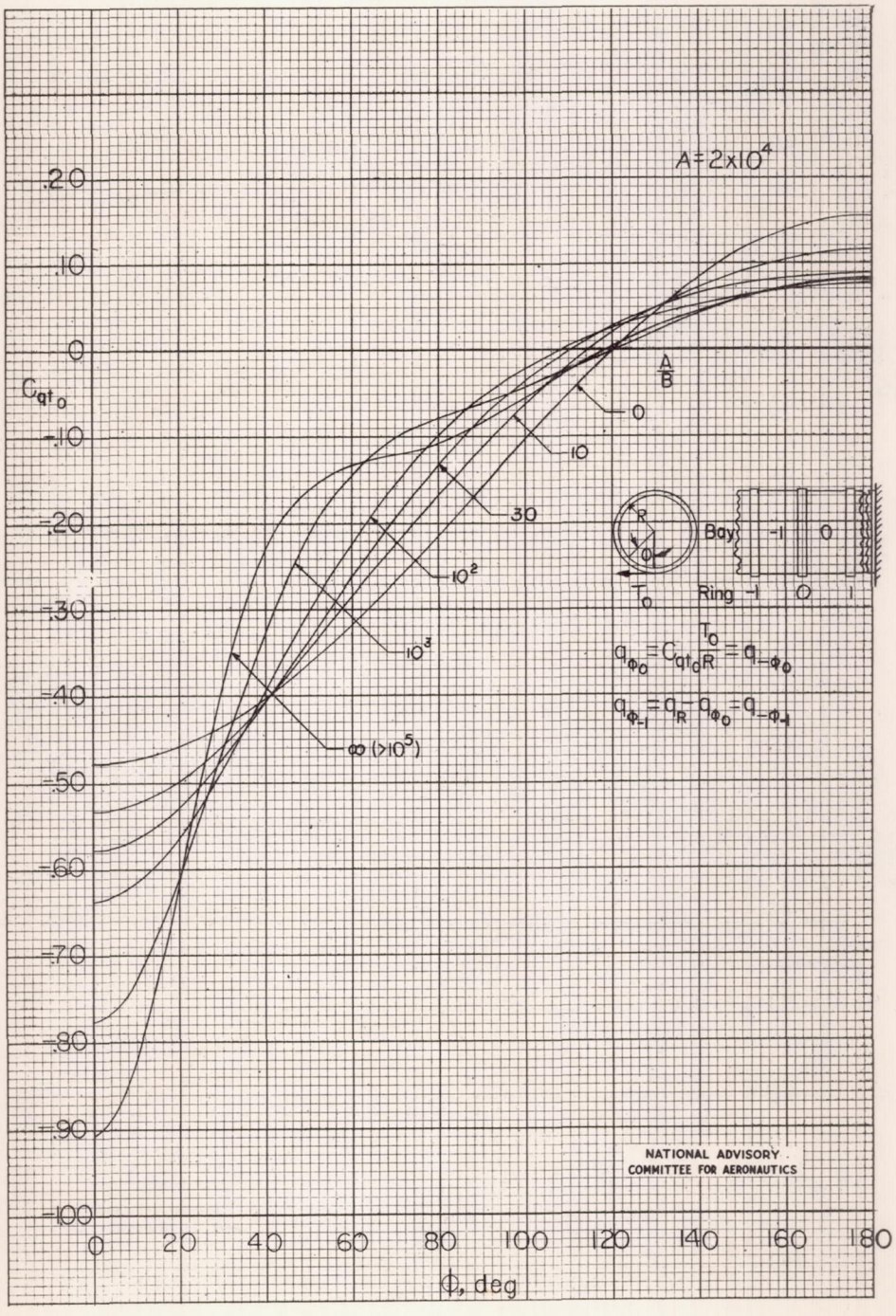

Figure 26.- Skin shear-flow coefficients for tangential load. ($A = 2 \times 10^4$.)

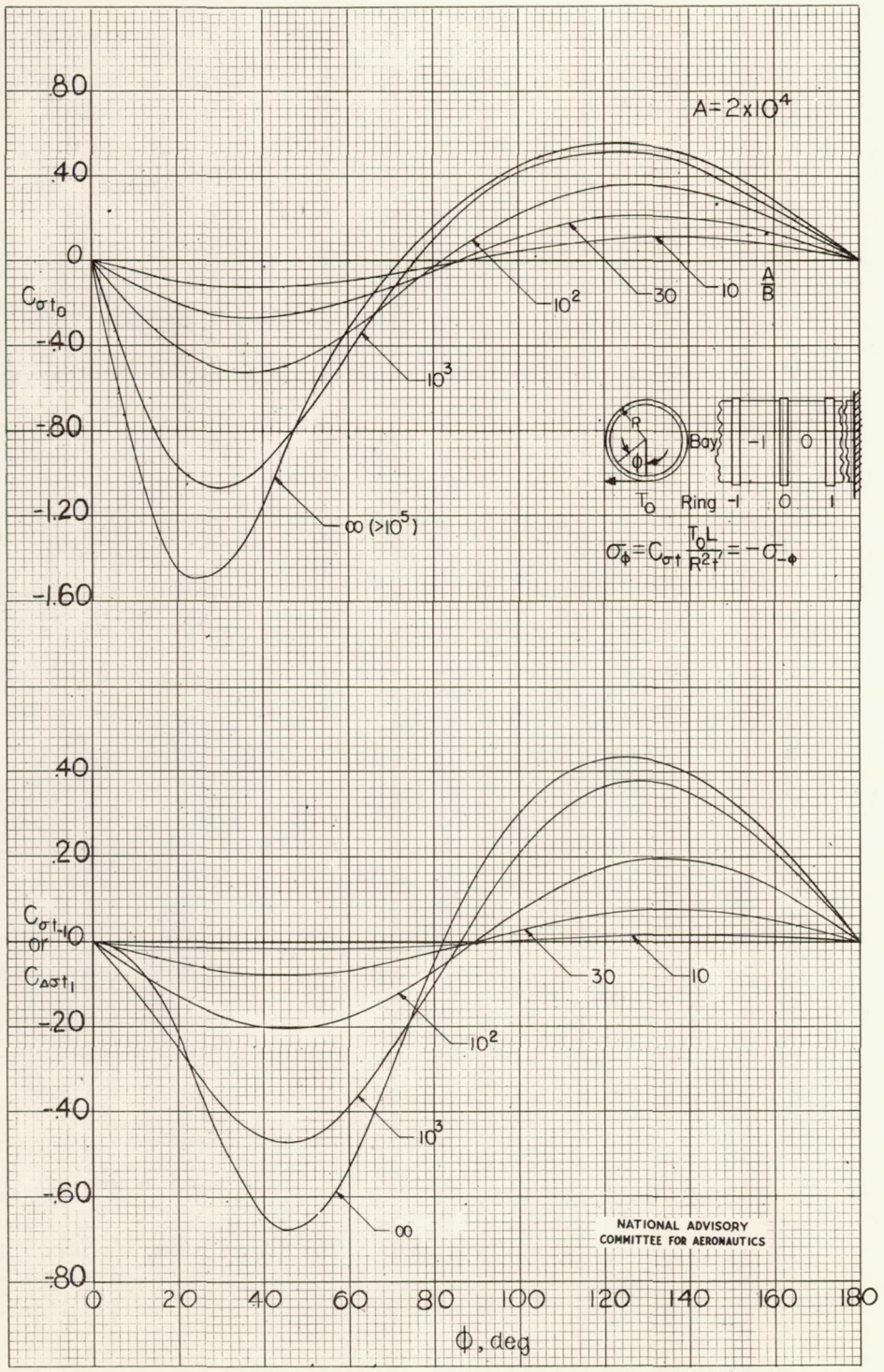

Figure 27.- Skin direct-stress coefficients at rings for tangential load. ($A = 2 \times 10^4$.)

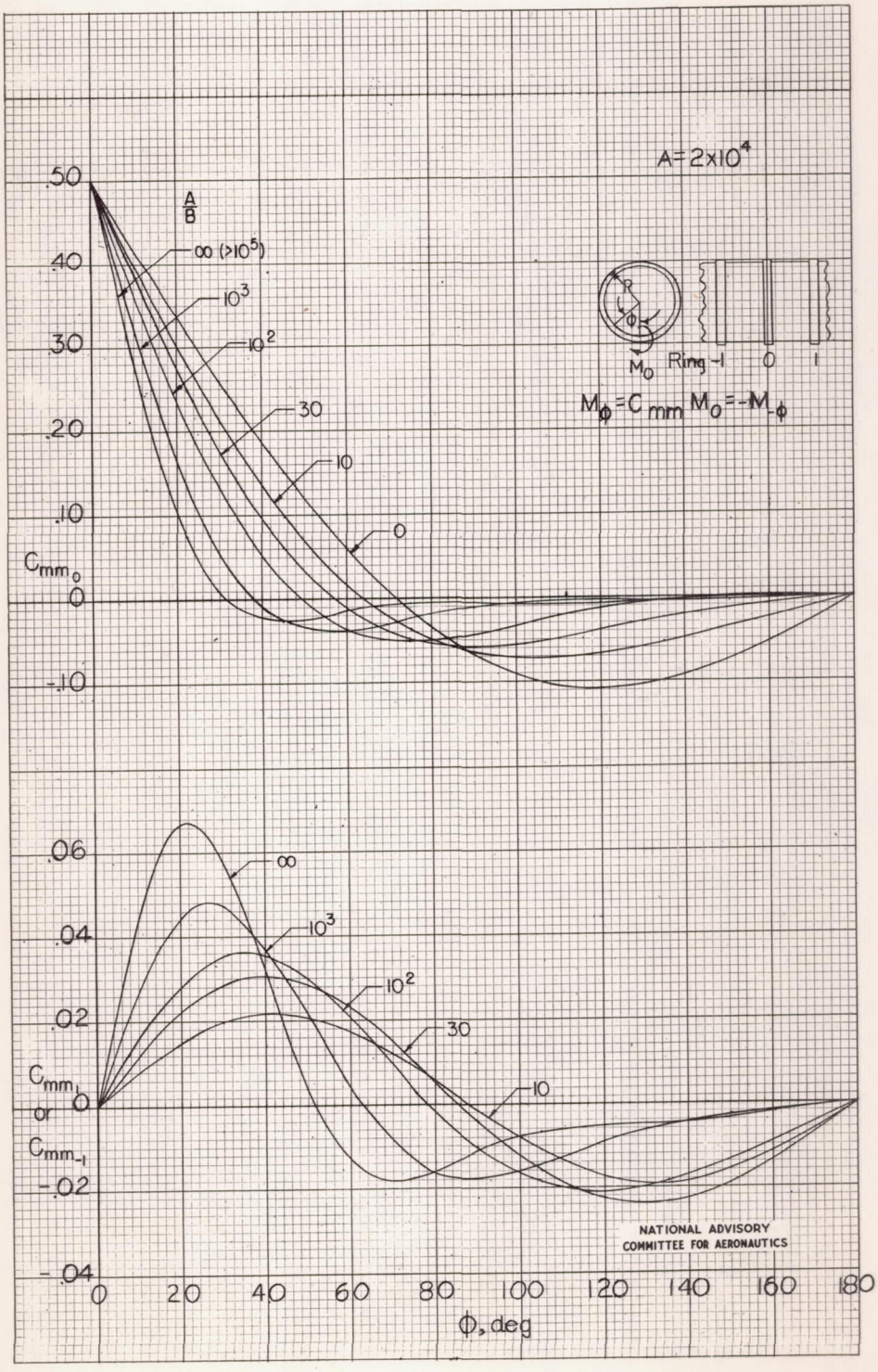

Figure 28.- Ring bending-moment coefficients for moment load. ($A = 2 \times 10^4$.)

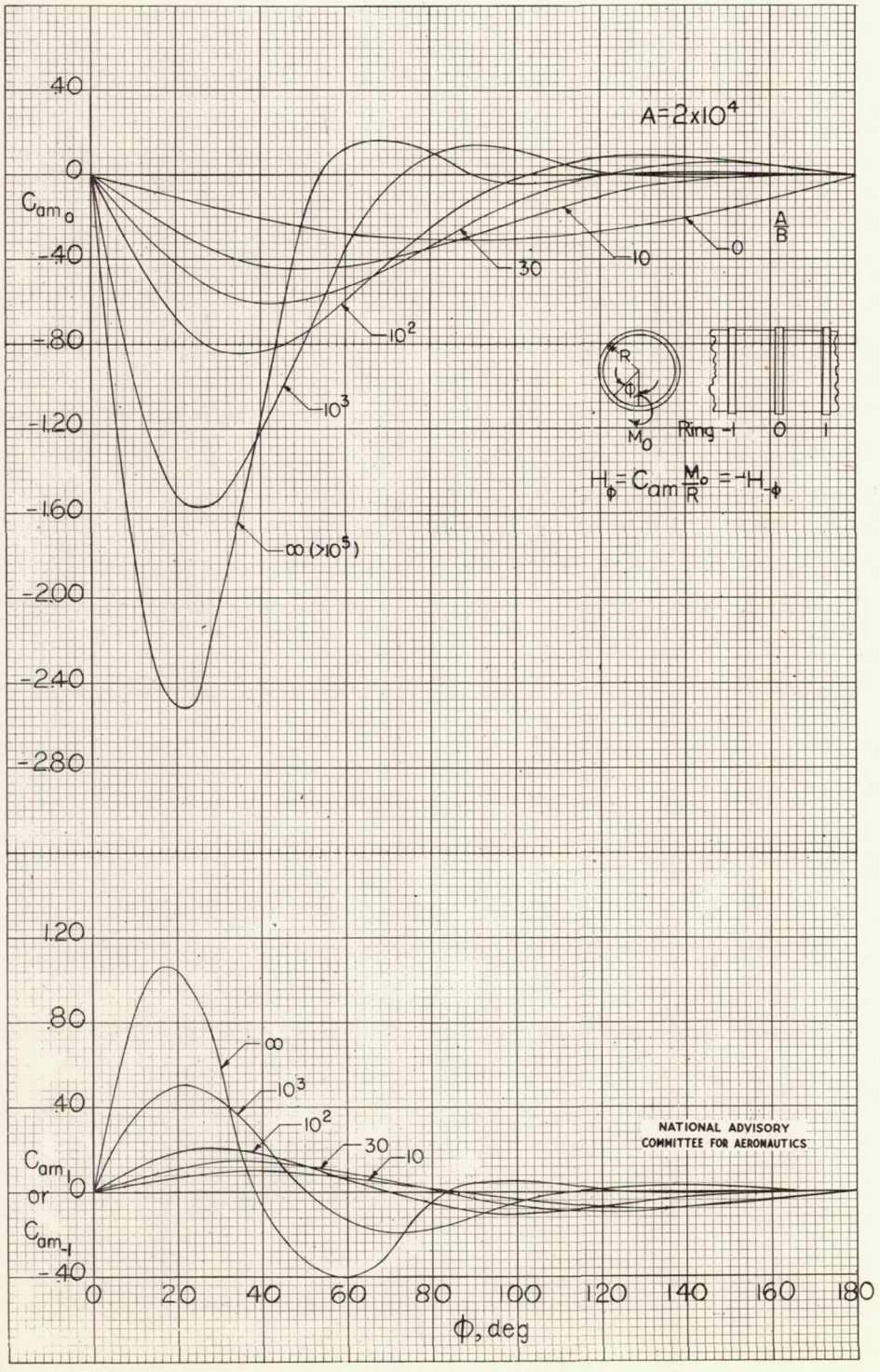

Figure 29.- Ring axial-load coefficients for moment load. ($A = 2 \times 10^4$.)

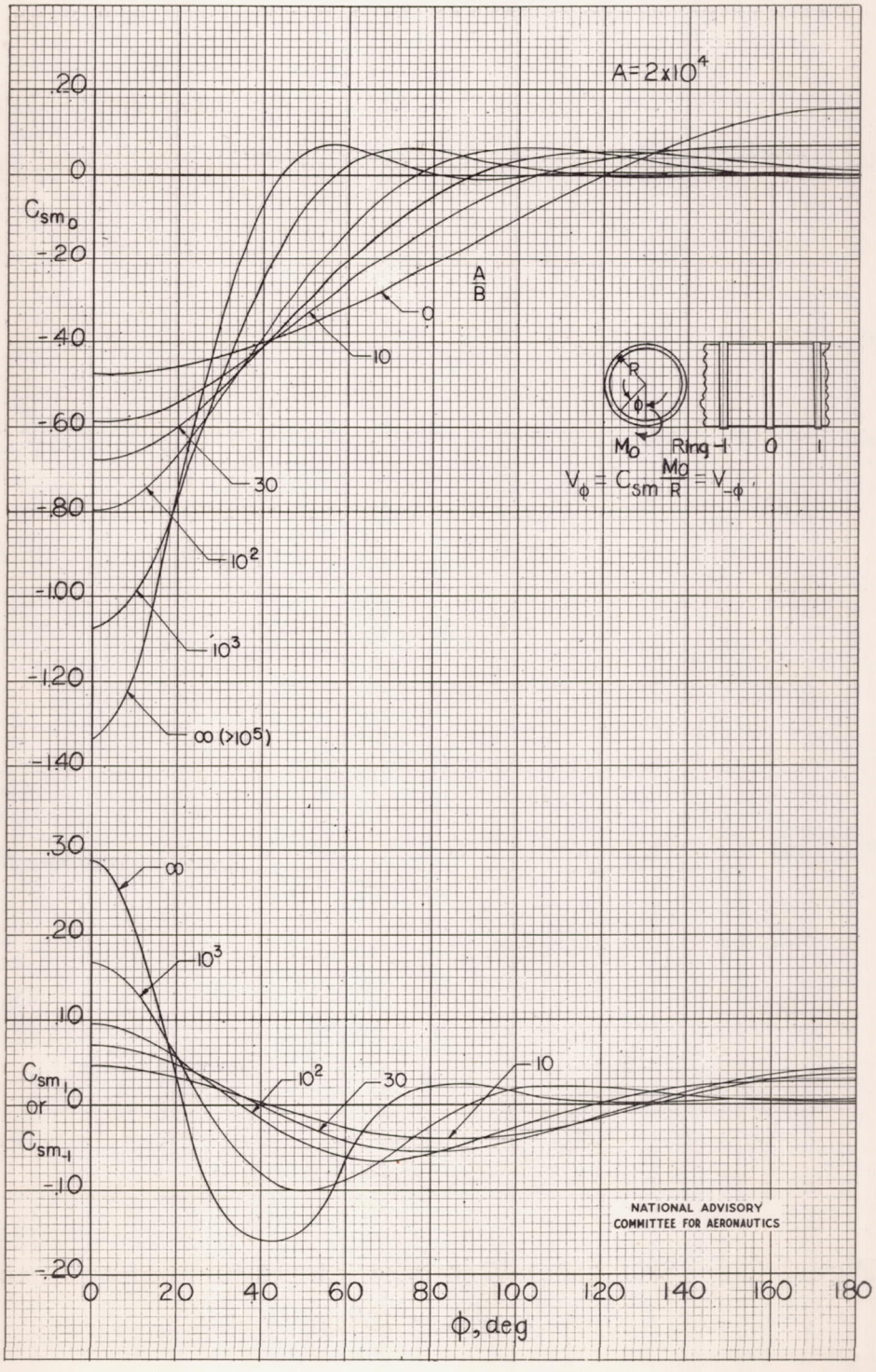

Figure 30.- Ring transverse-shear coefficients for moment load. ($A = 2 \times 10^4$.)

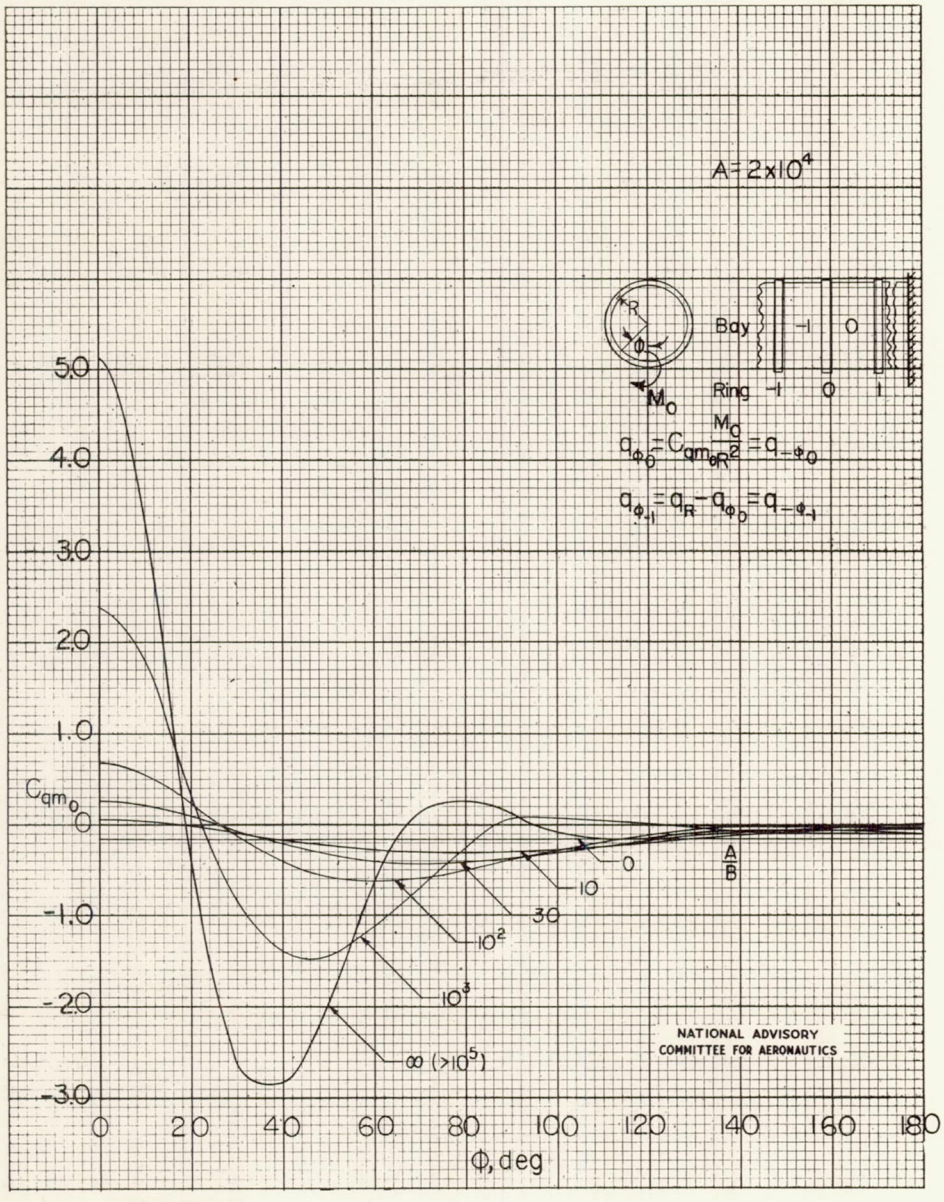

Figure 31.- Skin shear-flow coefficients for moment load. ($A = 2 \times 10^4$.)

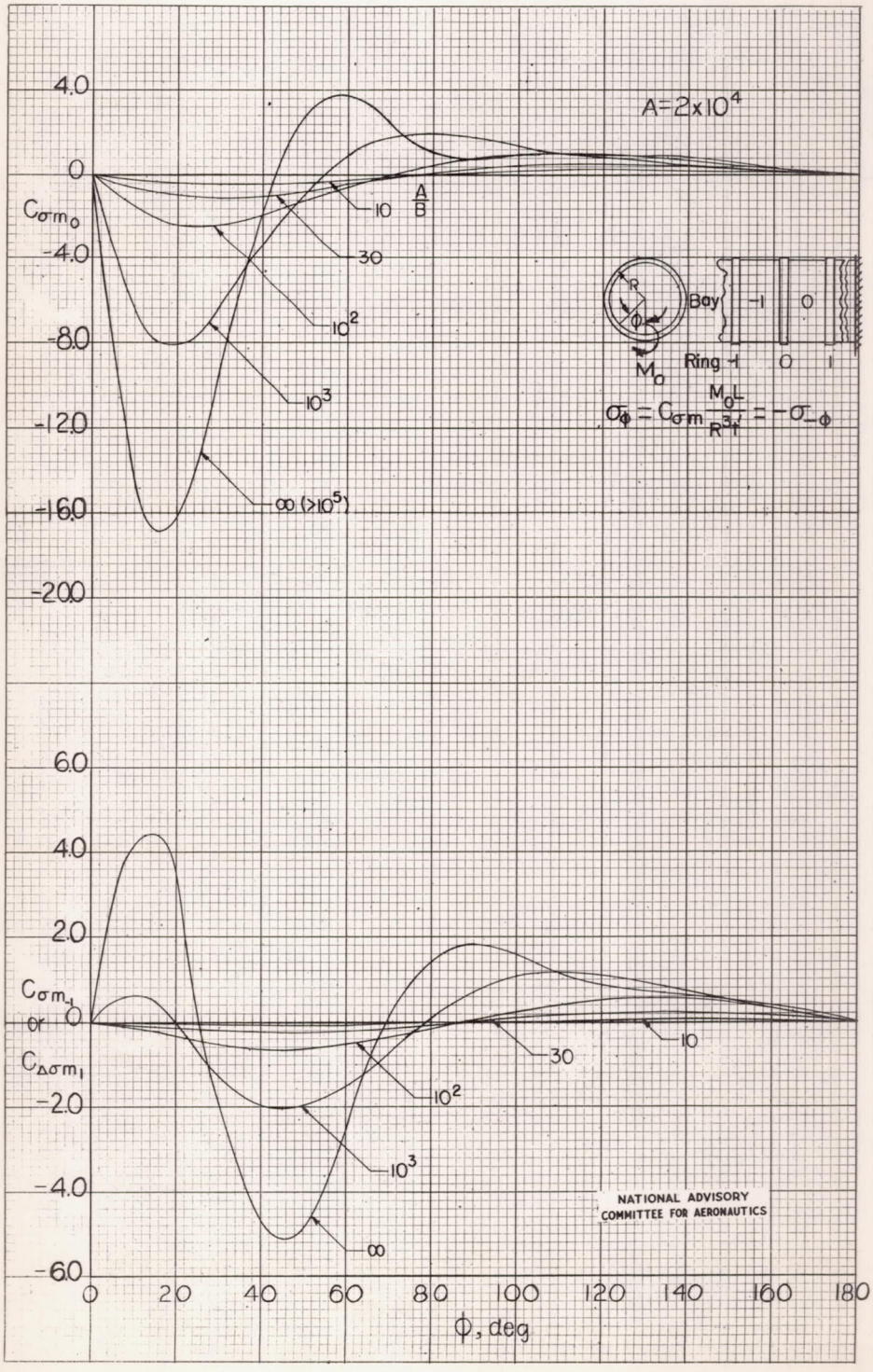

Figure 32.- Skin direct-stress coefficients at rings for moment load. ($A = 2 \times 10^4$.)

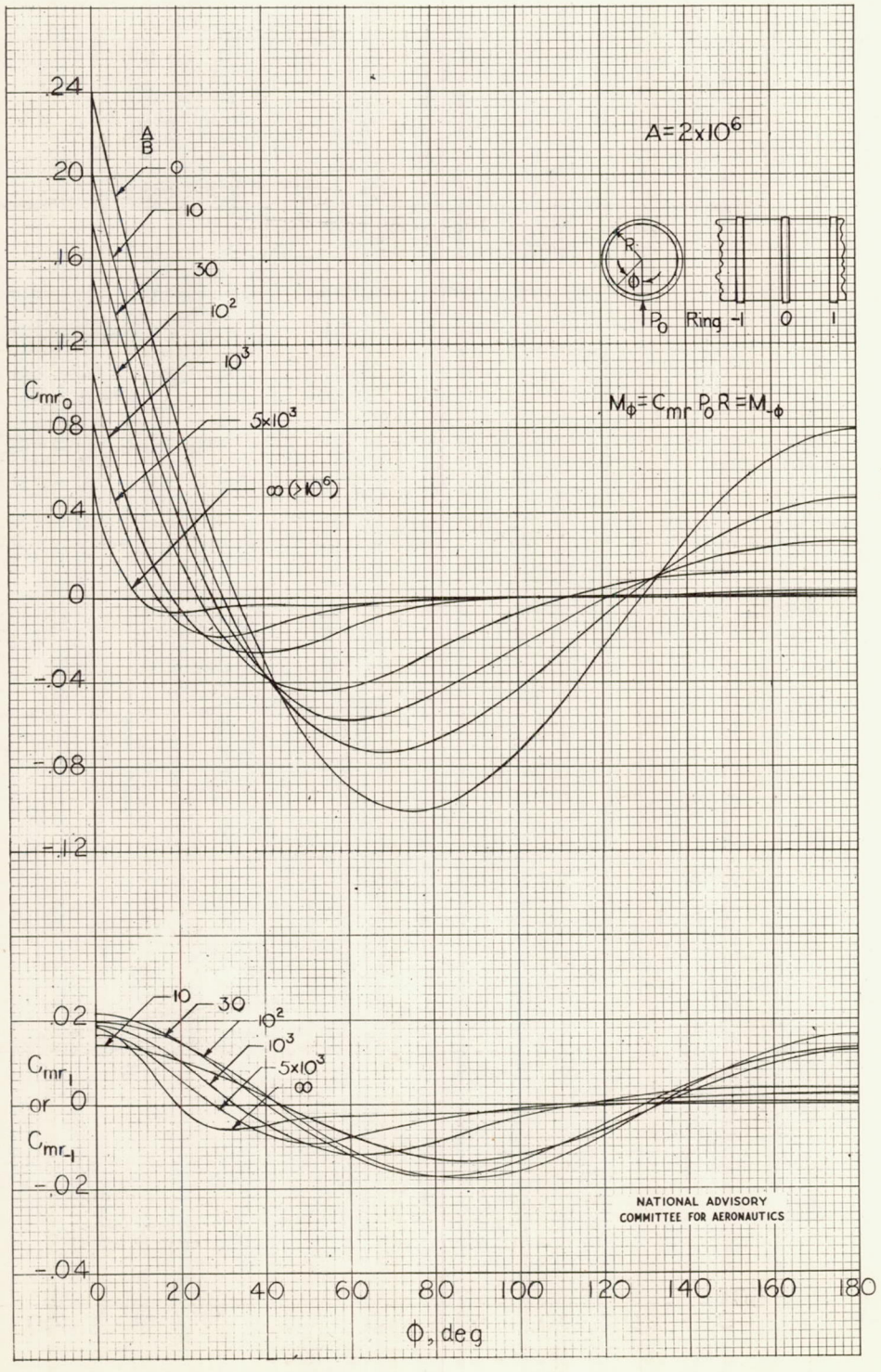

Figure 33.- Ring bending-moment coefficients for radial load. ($A = 2 \times 10^6$.)

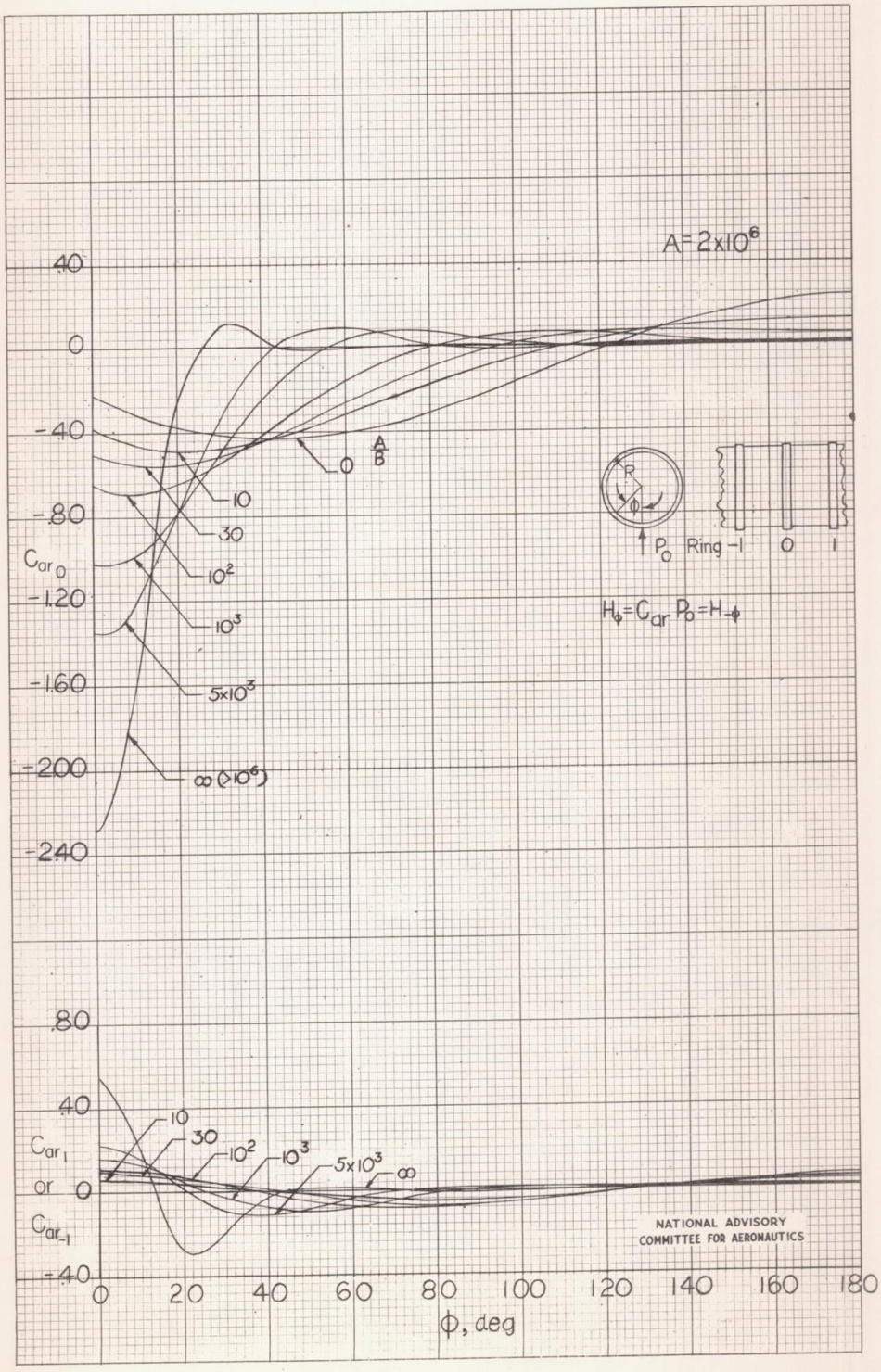

Figure 34.- Ring axial-load coefficients for radial load. ($A = 2 \times 10^6$.)

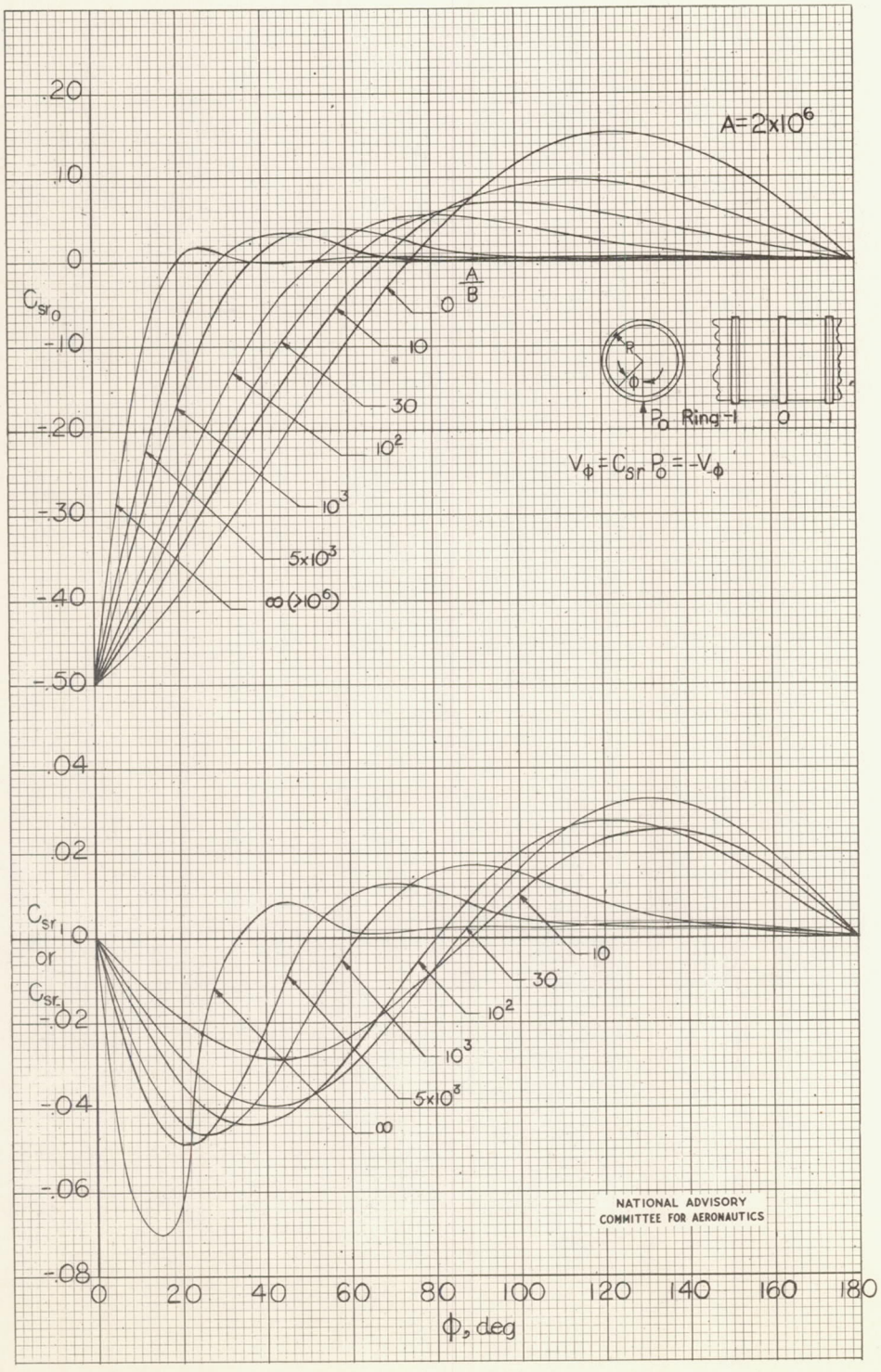

Figure 35.- Ring transverse-shear coefficients for radial load. ($A = 2 \times 10^6$.)

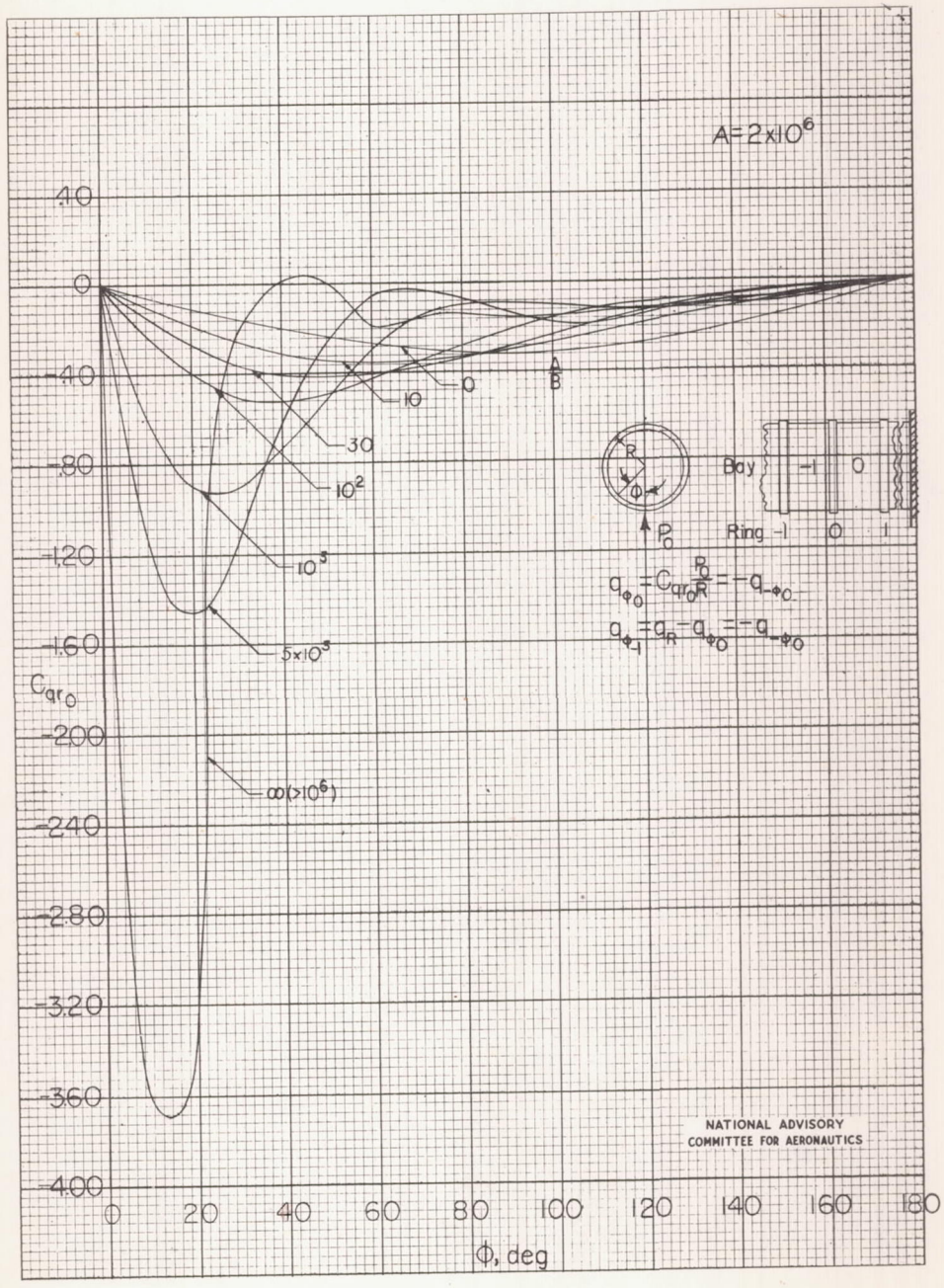

Figure 36.- Skin shear-flow coefficients for radial load. ($A = 2 \times 10^6$.)

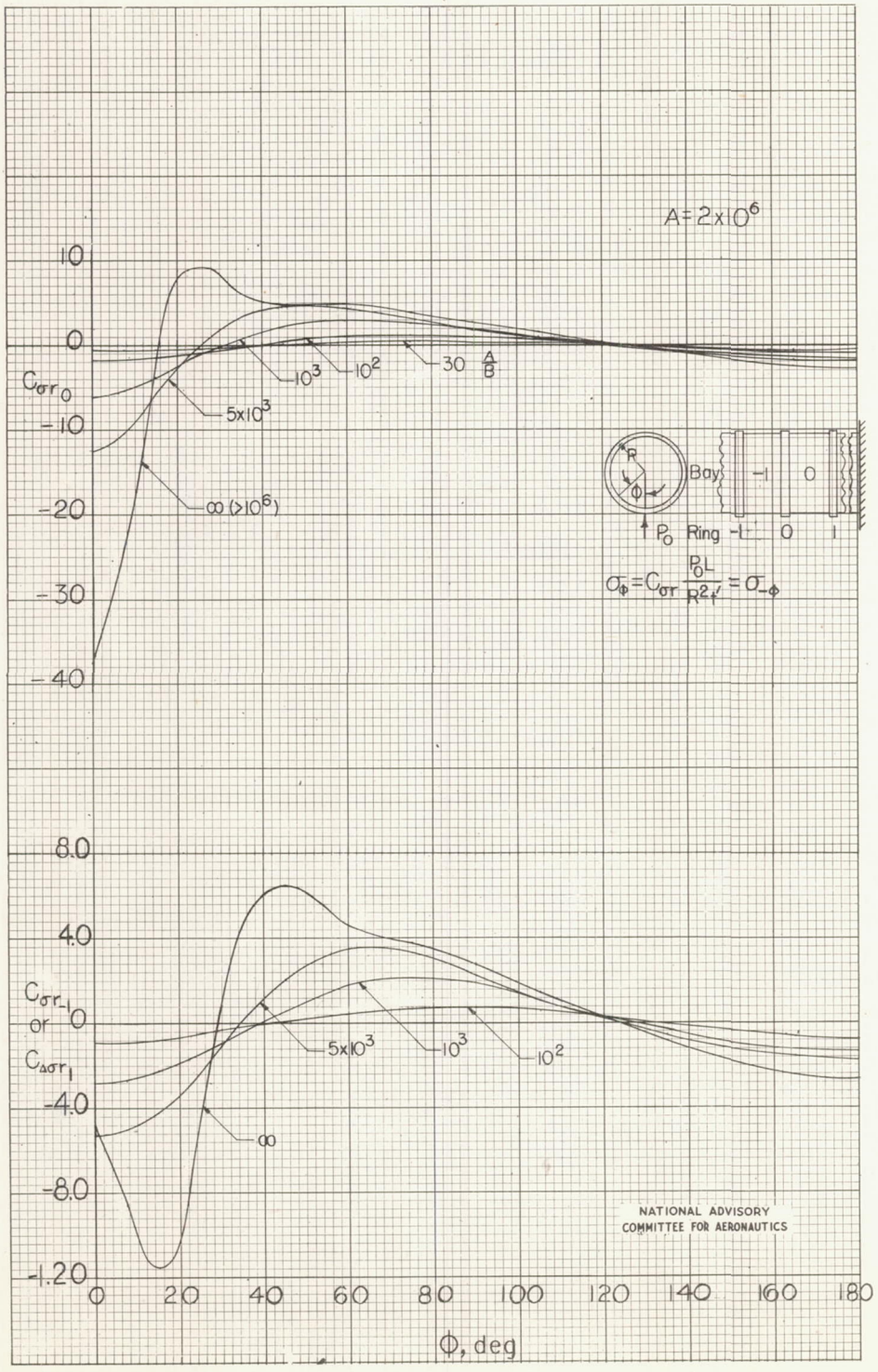

Figure 37.- Skin direct-stress coefficients at rings for radial load. (A = 2 × 10^6.)

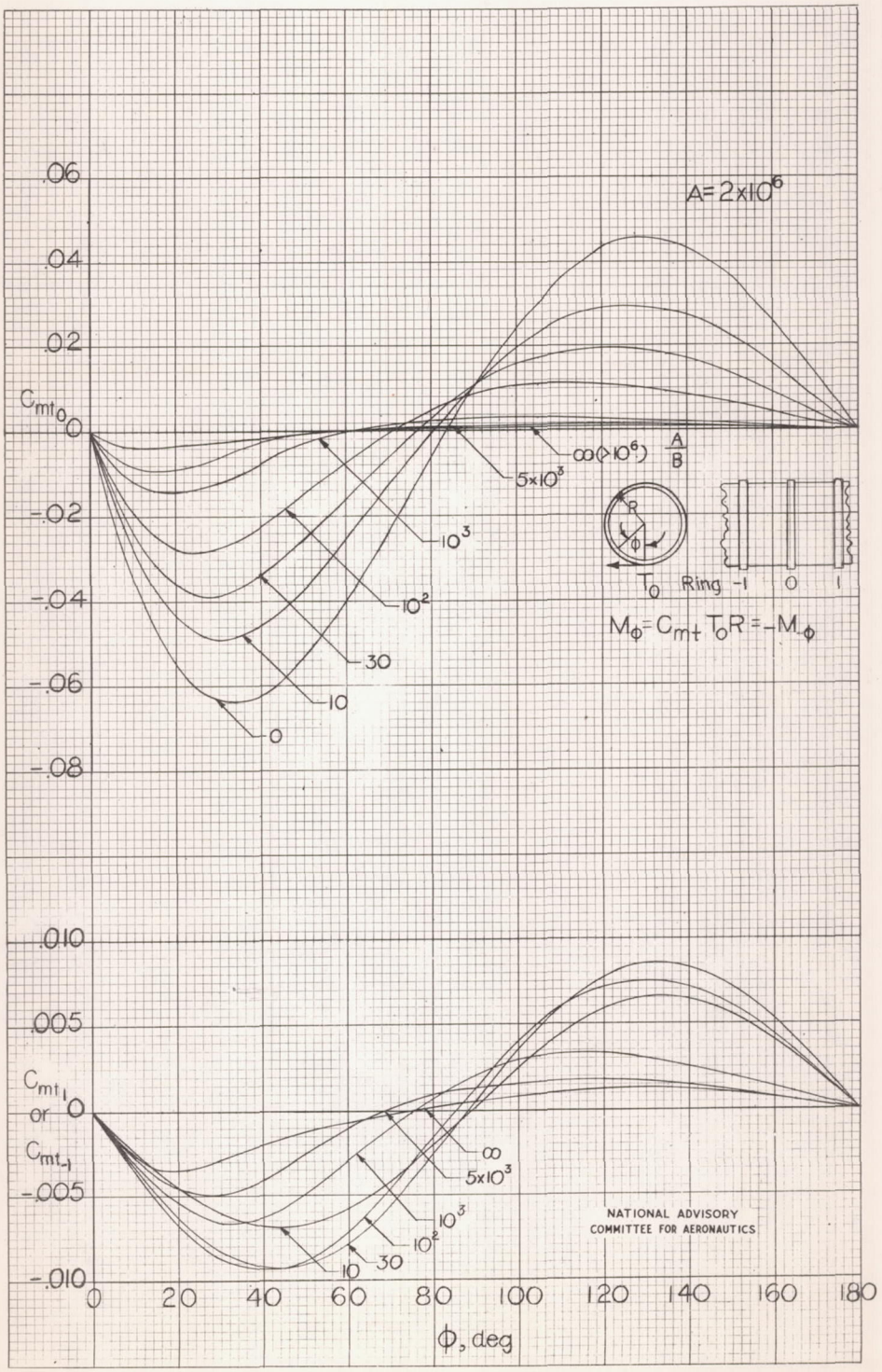

Figure 38.- Ring bending-moment coefficients for tangential load. ($A = 2 \times 10^6$.)

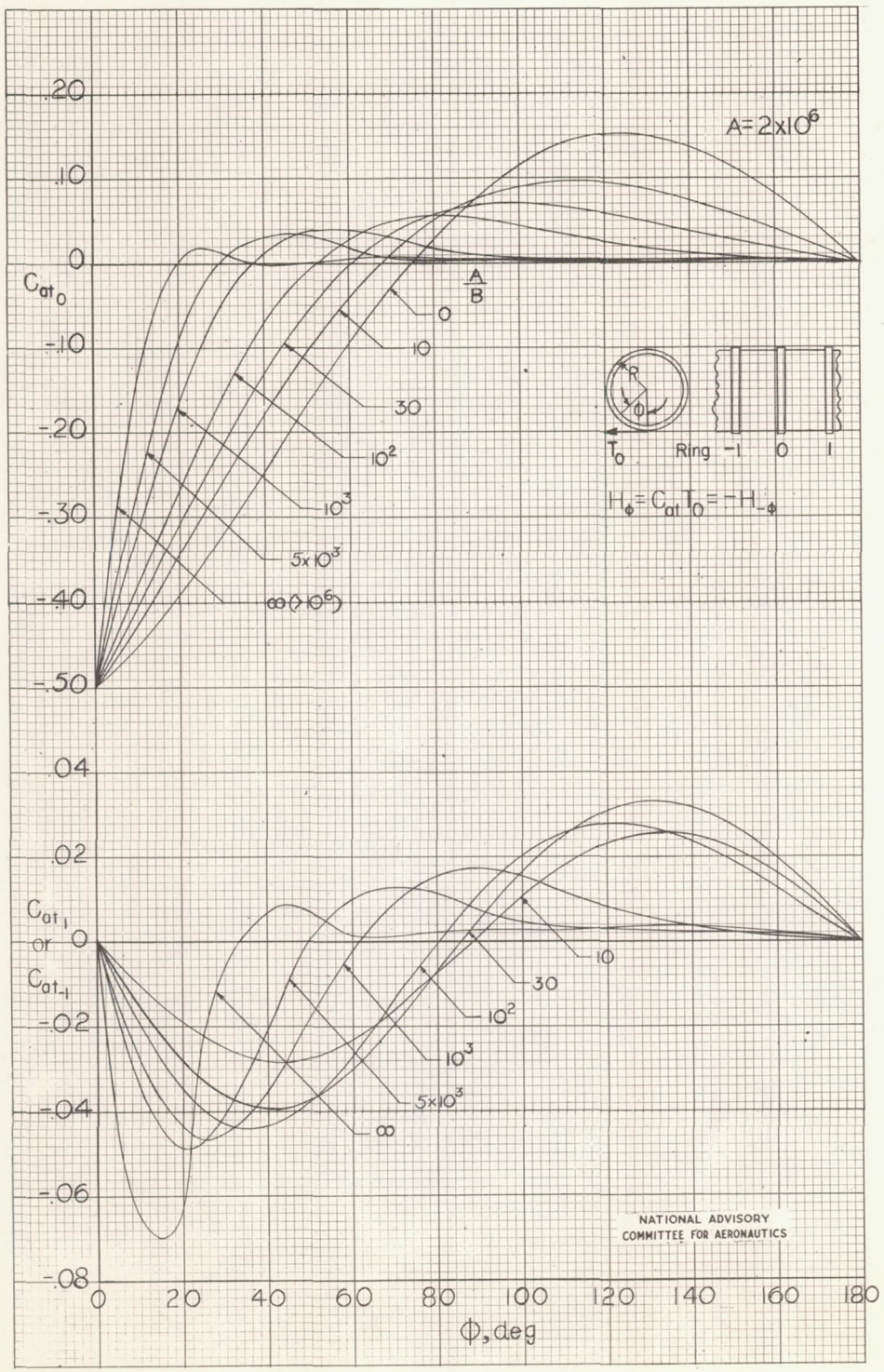

Figure 39.- Ring axial-load coefficients for tangential load. ($A = 2 \times 10^6$.)

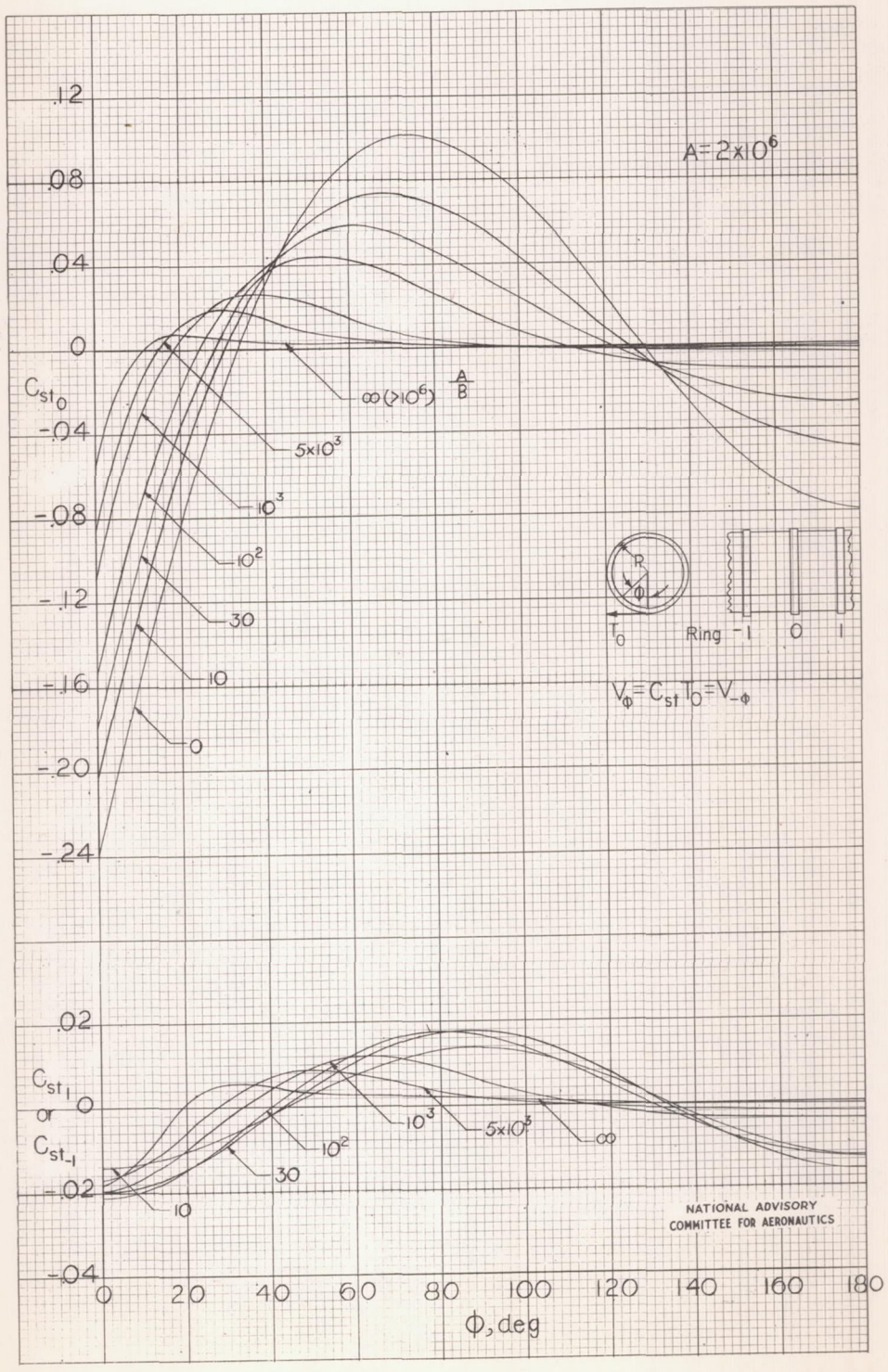

Figure 40.- Ring transverse-shear coefficients for tangential load. ($A = 2 \times 10^6$.)

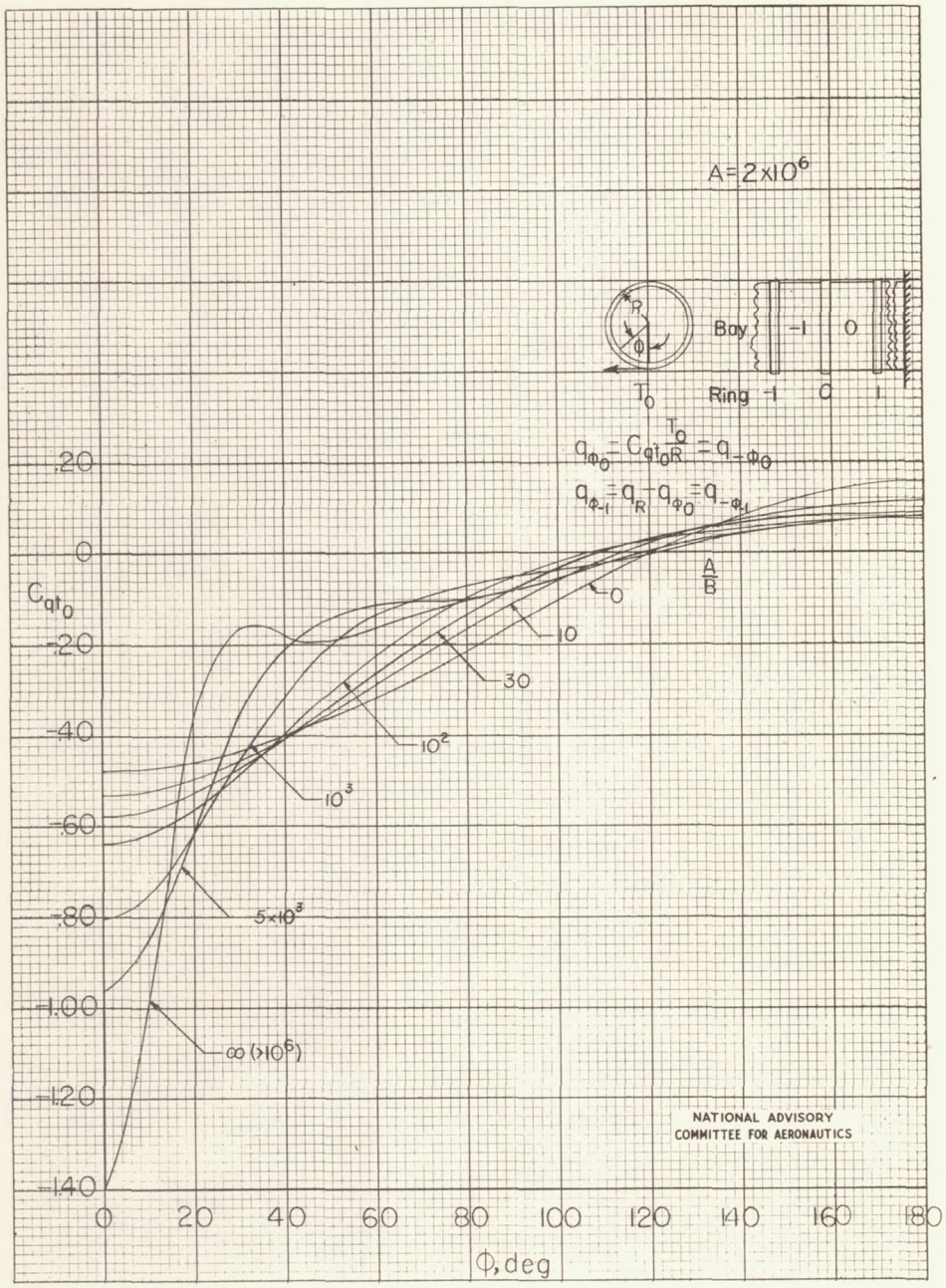

Figure 41.- Skin shear-flow coefficients for tangential load.
($A = 2 \times 10^6$.)

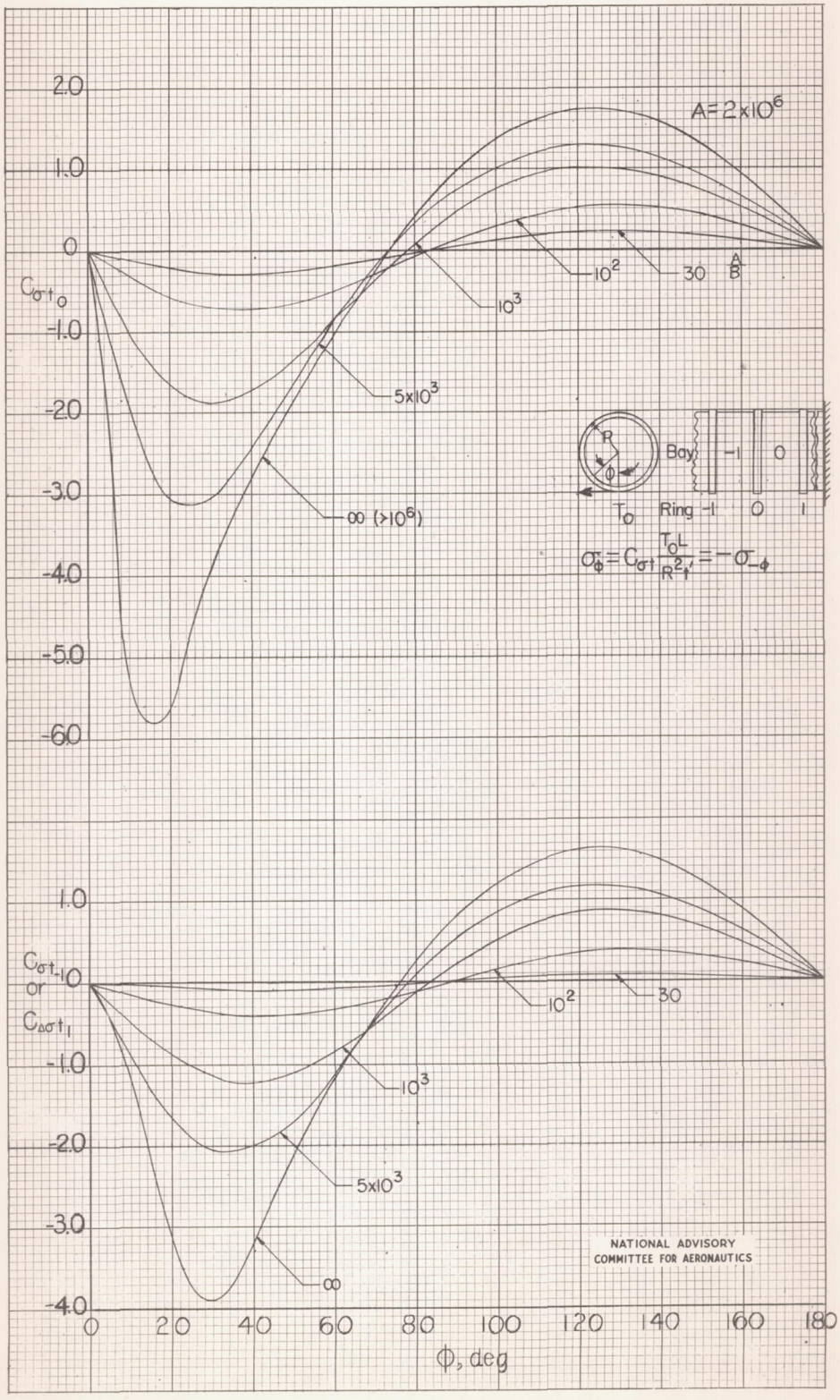

Figure 42.- Skin direct-stress coefficients at rings for tangential load. ($A = 2 \times 10^6$.)

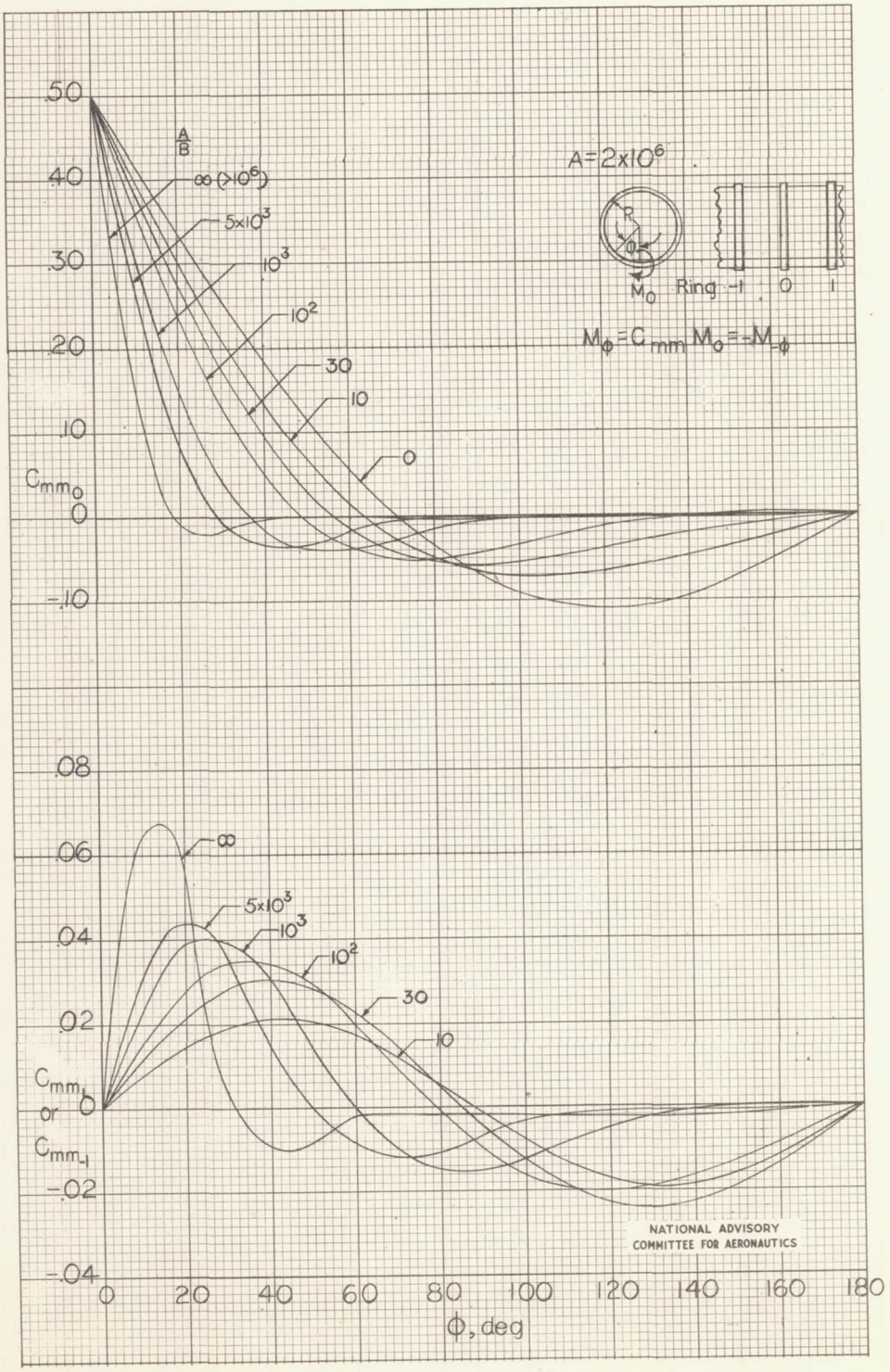

Figure 43.- Ring bending-moment coefficients for moment load. ($A = 2 \times 10^6$.)

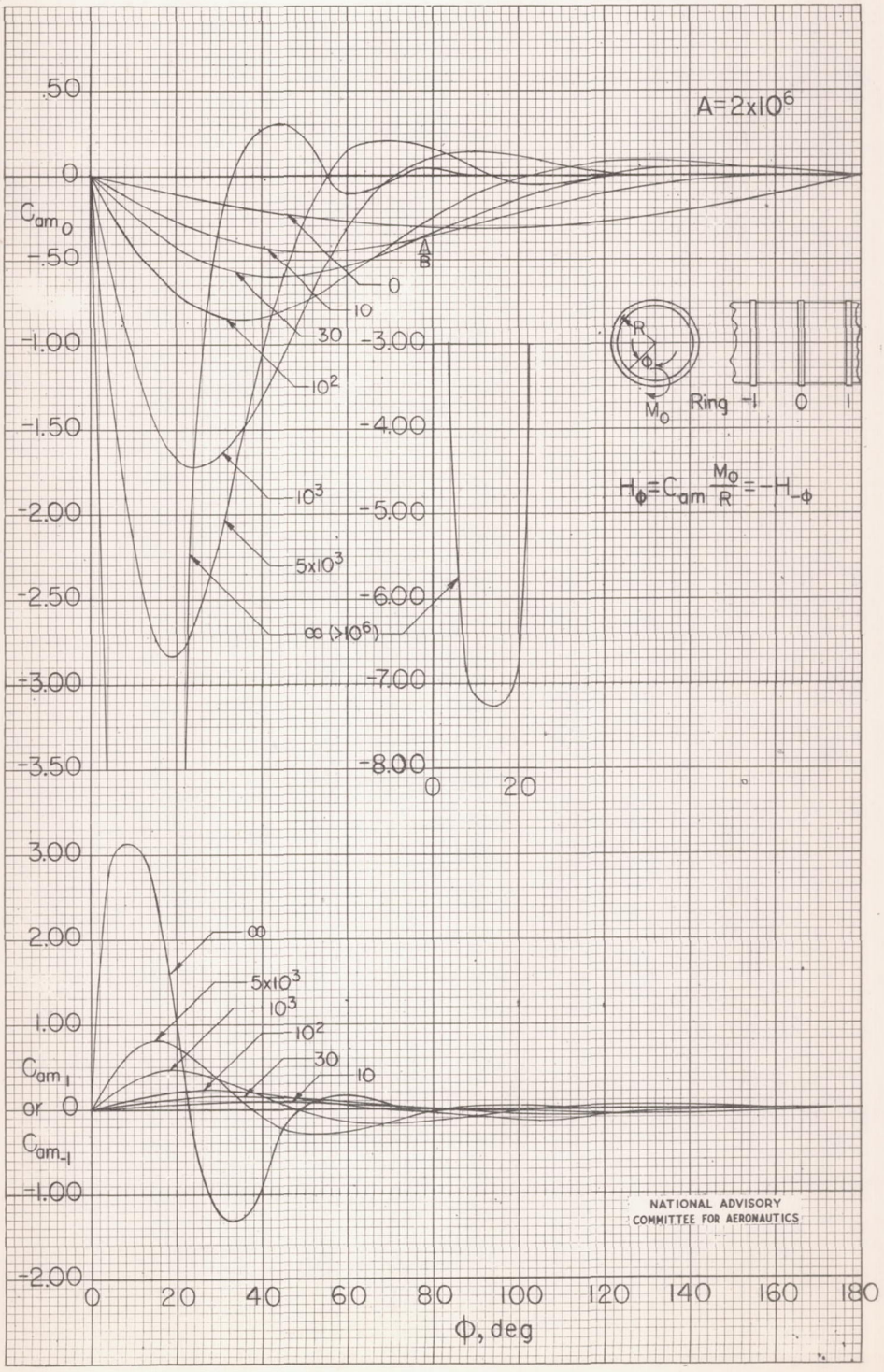

Figure 44.- Ring axial-load coefficients for moment load. ($A = 2 \times 10^6$.)

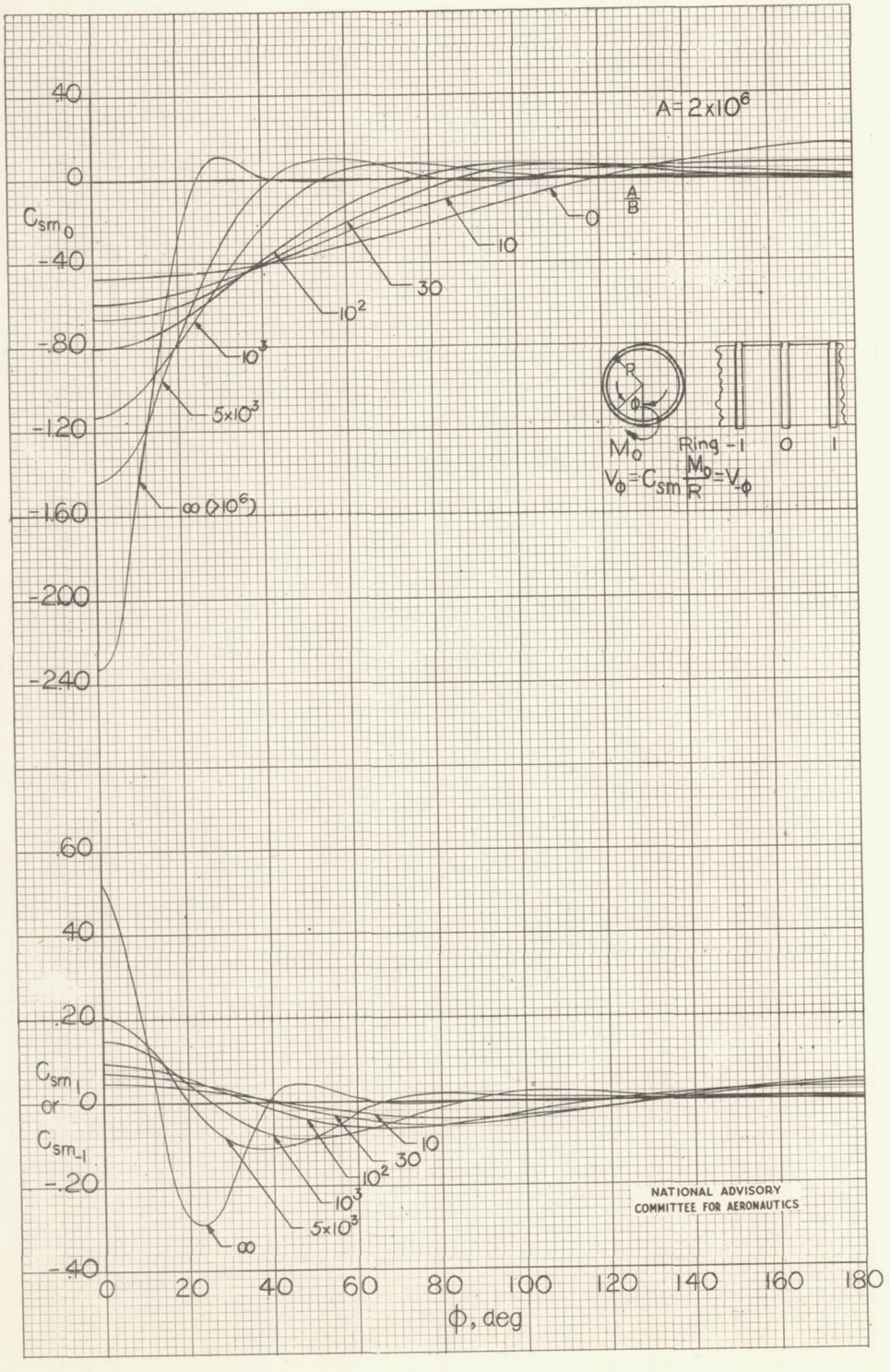

Figure 45.- Ring transverse-shear coefficients for moment load. ($A = 2 \times 10^6$.)

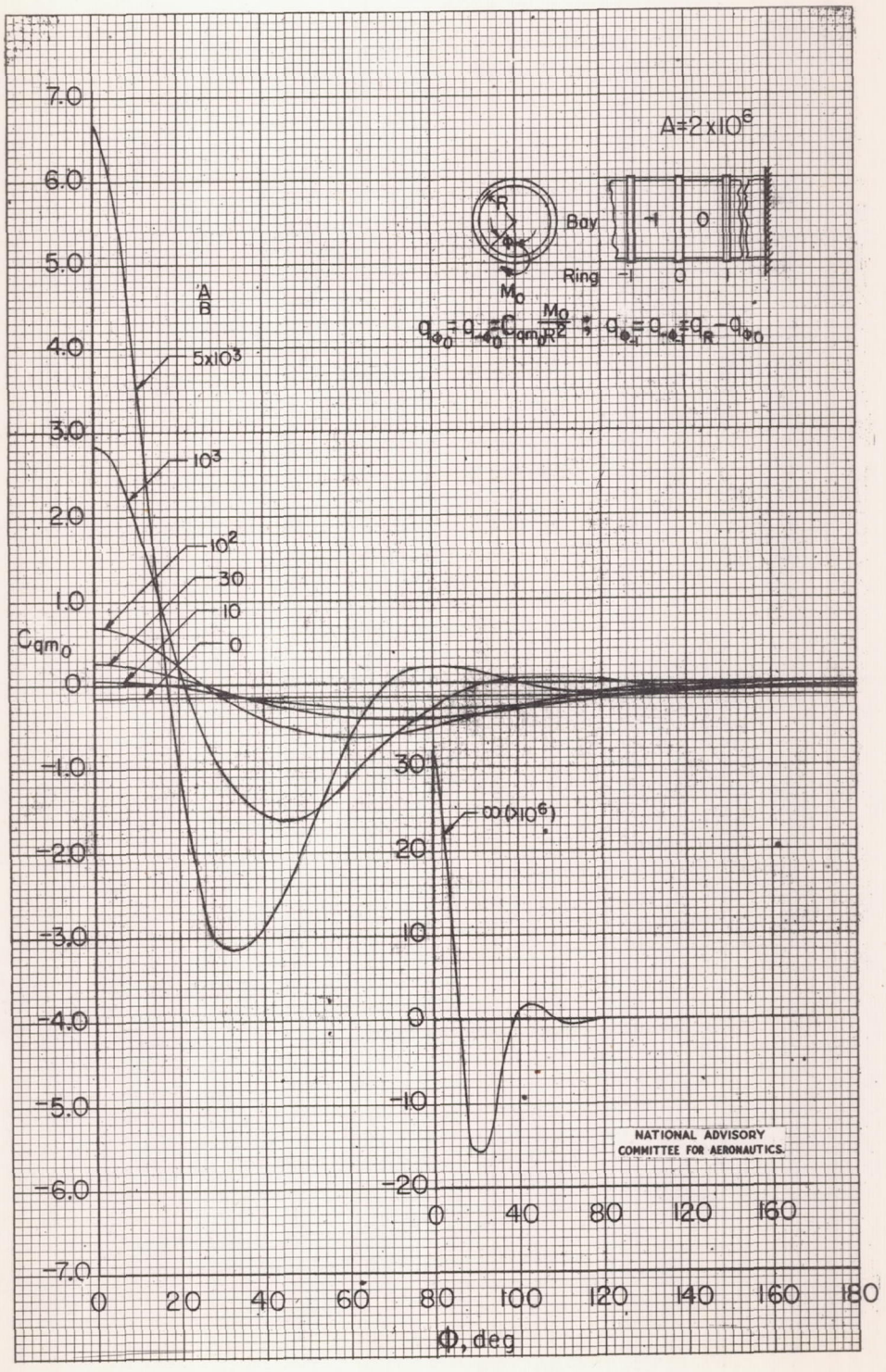

Figure 46.- Skin shear-flow coefficients for moment load. ($A = 2 \times 10^6$.)

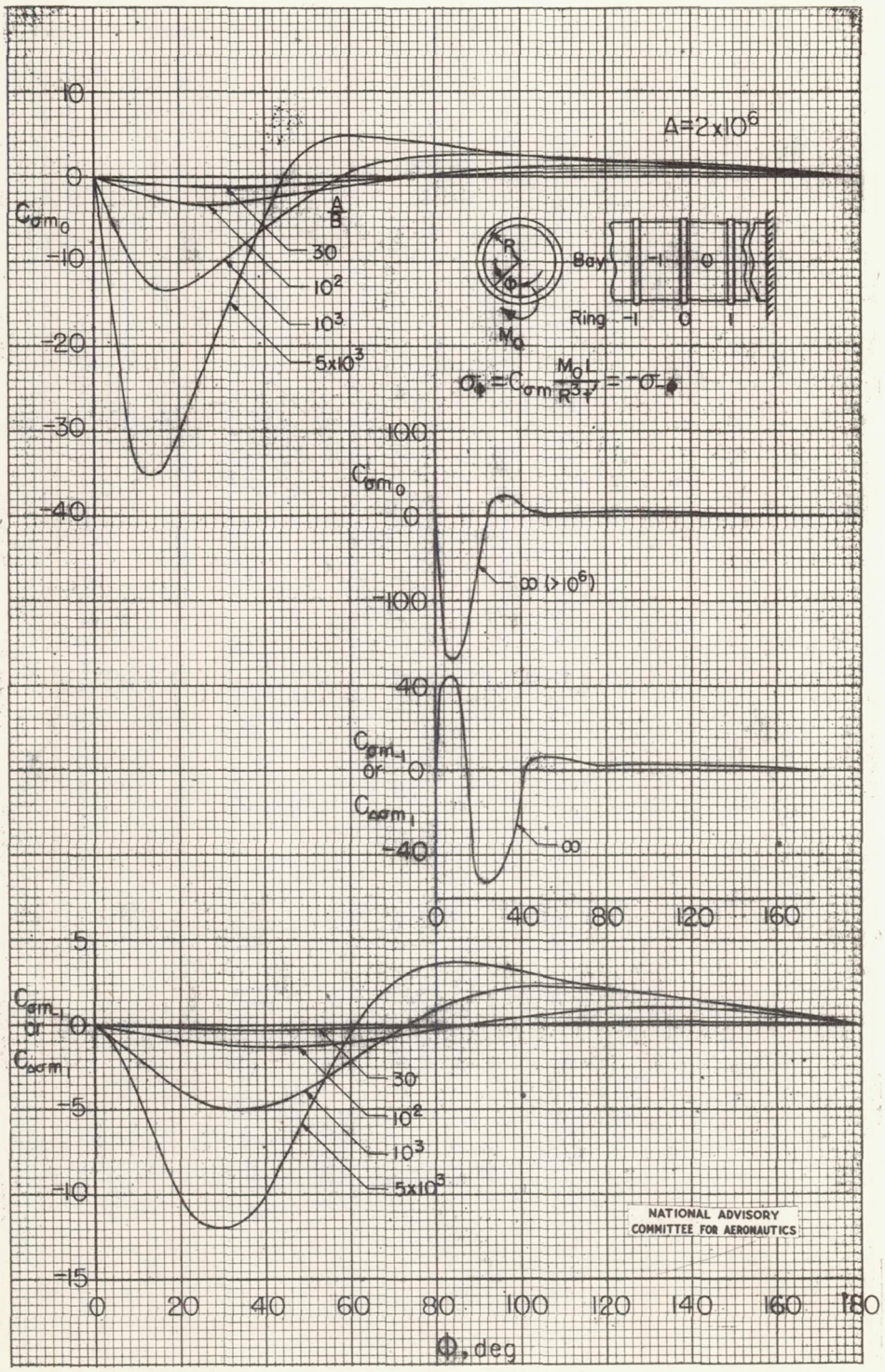

Figure 47.- Skin direct-stress coefficients at rings for moment load. ($A = 2 \times 10^6$.)

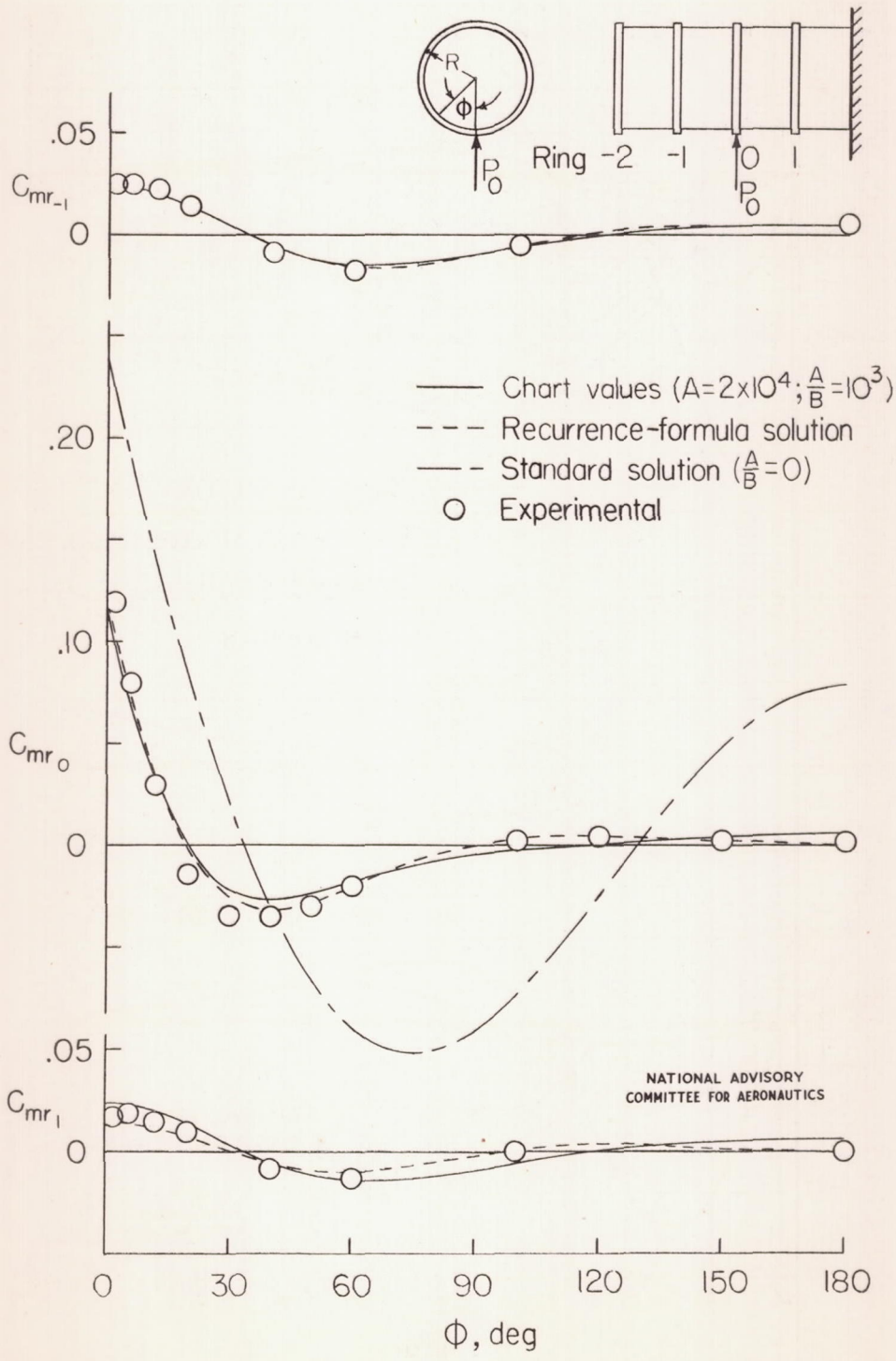

Figure 48.- Comparison among calculated and experimental ring bending-moment coefficients for cantilevered cylinder.

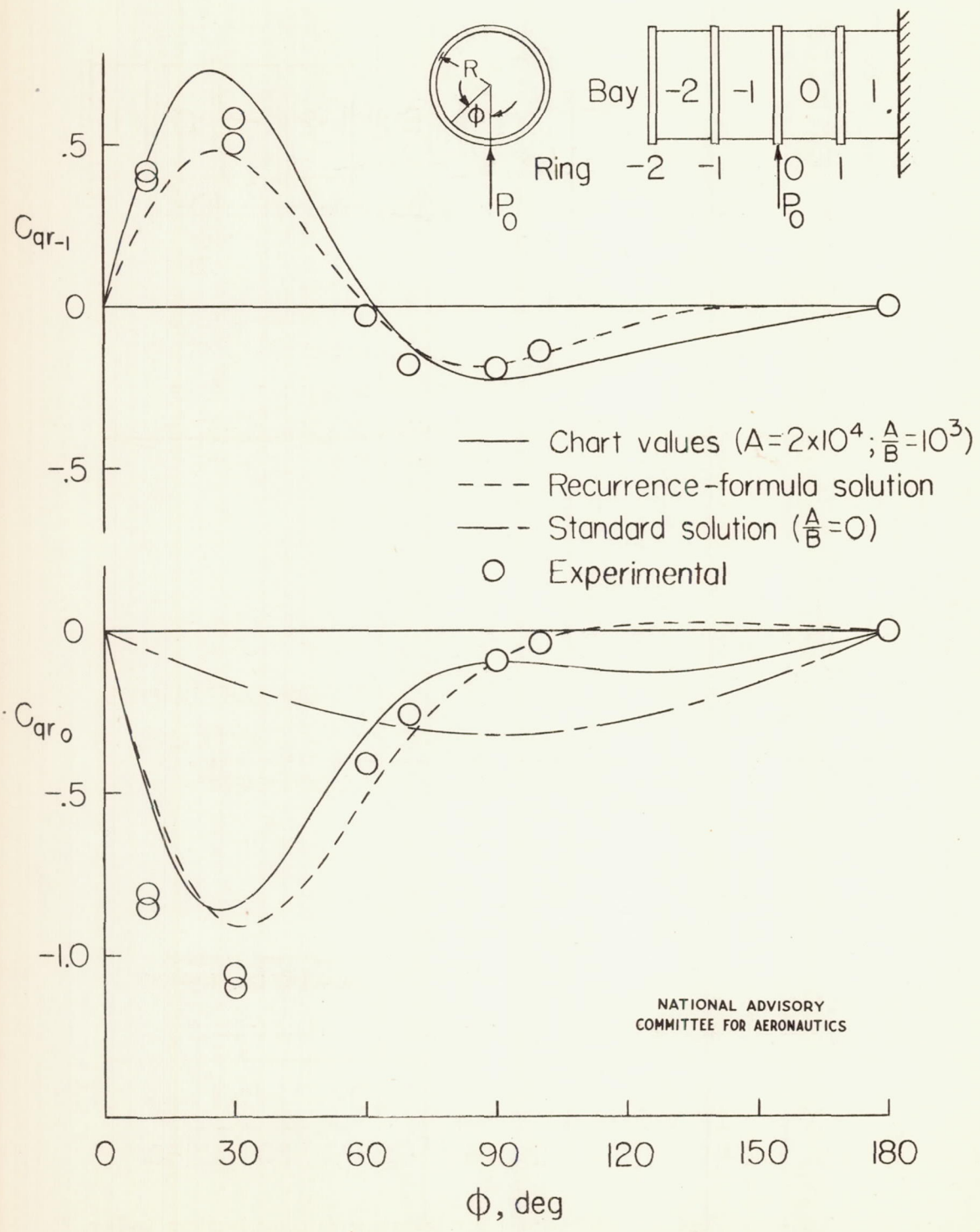

Figure 49.- Comparison among calculated and experimental skin shear-flow coefficients for cantilevered cylinder.

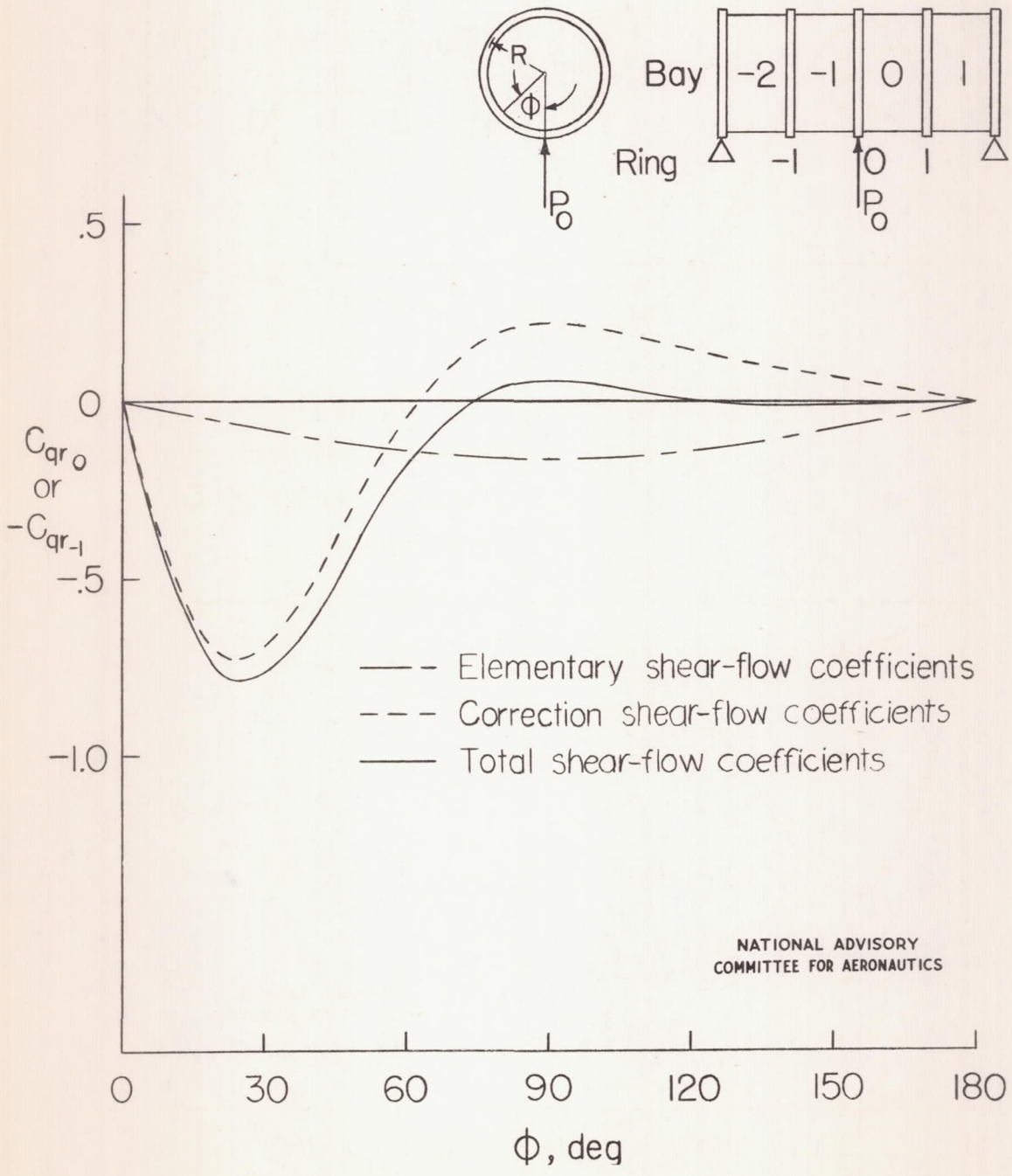

Figure 50.- Shear-flow coefficients for simply supported cylinder.